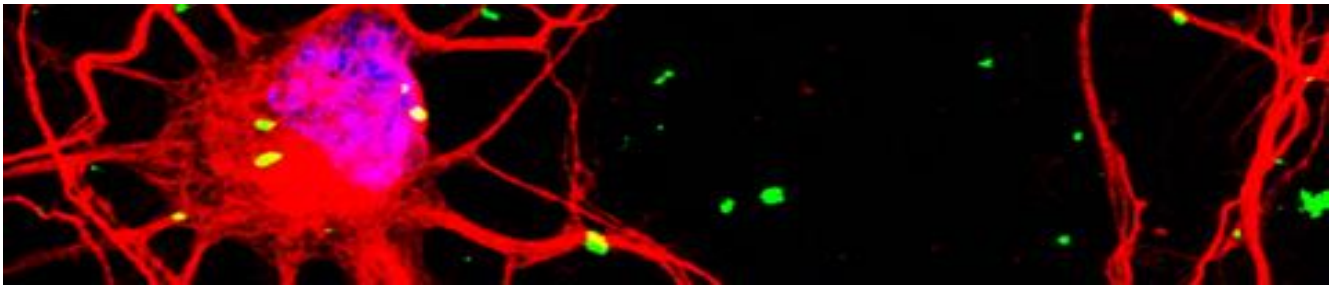

Corso di Dottorato in Neuroscienze
Curriculum Neuroscienze e Neurotecnologie
Ciclo XXXI

# Characterization of the Kidins220 CaMKII-Cre conditional KO mouse line


**Author: Amanda Almacellas Barbanoj**

**Supervisor: Fabrizia Cesca, PhD**


ISTITUTO ITALIANO DI TECNOLOGIA

UNIVERSITÀ DEGLI STUDI DI GENOVA

# Abstract

Kidins220 (*Kinase-D interacting substrate of 220 kDa*) is a scaffold transmembrane protein abundantly expressed in the nervous system. Mutations in the KIDINS220 gene have been correlated with psychiatric disorders and with the recently described SINO syndrome, characterized by spastic paraplegia, intellectual disability, syntagmus and obesity. Kidins220 is involved in several neuronal functions regulated by neurotrophic factors, including neuronal survival, differentiation and synaptic plasticity. Previous work with the complete KO mouse model for Kidins220 evidenced the crucial role of this protein in neuronal and cardiovascular development since its embryonic ablation is lethal. Thus to gain a comprehensive understanding of the role of Kidins220 in the adult mouse, a Cre/loxP based conditional KO (cKO) mouse model was generated, in which the $Ca^{2+}$/ Calmodulin-dependent kinase-II (CaMKII) promoter drives Cre expression, and consequently protein deletion specifically in the postnatal forebrain. The characterization of the Kidins220 cKO model has been accomplished through diverse approaches: behavioural experiments, brain and neuron morphological analysis, molecular signalling from brain slices and cultures, protein and gene expression assessment. cKO mice display alterations in anxiety levels and social behaviour, with a clear impairment in social memory. At the morphological level, data show reduced dendritic branching in cortical and hippocampal neurons, while at the molecular level, neuronal response to brain-derived neurotrophic factor (BDNF) stimulation is blunted, as well as the mitogen-activated protein kinase (MAPK) pathway activation. The behavioural profile of these animals provides useful knowledge about the pathophysiology of Kidins220, indicating that alterations of this protein expression may have important consequences on human pathologies of the cognitive and social sphere. Some psychiatric diseases are highly inheritable, and their causes have been traced back to genetic alterations such as point mutations and epigenetic modifications. A better understanding of such inheritable traits will provide us with a better knowledge of the cellular and physiological alterations underlying the behavioural and cognitive symptomatology of patients. In this respect, the knowledge of Kidins220 function will contribute to further elucidate the

neuropathological mechanisms underlying some psychiatric diseases.

# Contents

# I Introduction

## I.I Kidins220

Kidins220 (Kinase D-interacting substrate of 220kDa) / ARMS (Ankyrin repeat-rich membrane spanning), hereby referred to as Kidins220, was identified as the first physiological Kinase D substrate in neural cells [1] ] and as a novel downstream target of neurotrophin and ephrin receptor tyrosine kinases [2]. Kidins220 is a transmembrane scaffold protein ubiquitously expressed with a higher expression in the nervous system [1, 2]. Its sequence is highly conserved across species [2], enabling the study of Kidins220 with animal models. In the mouse nervous system, Kidins220 expression is modulated across development: the maximum protein expression occurs at birth and decreases over the first month, after which it remains constant [3]. Kidins220 is expressed in the entire mouse brain, with a more prominent concentration in the cortex and the hippocampus. Specifically, in the cortex, a high expression of this protein is found in pyramidal neurons of Layer 5 in both cell bodies and dendritic projections. In the hippocampus, it is found in the somas of the neurons of all hippocampal areas and in the dendrites of the molecular layer cells of the dentate gyrus [4].

## I.II Kidins220 structure and protein interactions

Kidins220 is a transmembrane scaffold protein comprised of multiple protein interaction domains (**Figure 1**), which are located in the N-terminal and C-terminal cytoplasmic tails, and in the four transmembrane domains [1].

### I.II.1 Ankyrin repeats

Ankyrin repeats are the most widely expressed protein motifs in nature and consist of 30-34 amino acid residues with the exclusive function of mediating protein-protein interactions [5]. The proteins which interact with Kidins220 via these domains are the following (see **Figure 1**):

**Trio:** this is a RhoGEF (guanine nucleotide exchange factor) that activates the GTPases (guanine triphosphatase) Rac1 and RhoG, which mediate cytoskeletal remodelling. Via its interaction with Kidins220, Trio promotes neurite outgrowth by activating these GTPases [6].

**MAP1b** (microtubule associated protein 1b): as its own name indicates, MAP1b is a factor that acts directly on microtubules to stabilize them. It is especially prominent in extending axons and their growth cones. Amongst its several functions, MAP1b modulates the stable anchoring of AMPA receptors to microtubules, and consequently their intracellular trafficking. Overexpression of MAP1B leads to a decrease in the number of AMPAR at the synapse [7]. Through its interaction with Kidins220, MAP1b regulates early axonal outgrowth and the establishment of neuronal polarity by modulating microtubule dynamics [8].

**SCG10** (superior cervical ganglion 10) and **Sclip** (Scgn10 like-protein): these are tubulin-regulating proteins of the stathmin family, exclusively expressed in the nervous system. They interact with Kidins220 in the perinuclear region and the growth cones, to facilitate the early stages of neural differentiation [9].

The specific interaction of Kidins220 with MAP1b and the two stathmin proteins and its ability to modify their activity place Kidins220 in a privileged position to coordinate their regulatory role on microtubule dynamics during neuronal polarization and development [9].

### I.II.2 Transmembrane domains

Kidins220 transmembrane domains allow its interaction with tropomyosin-related kinase (Trk) receptors [2].

**TrkA**: Kidins220 interacts with this receptor upon nerve growth factor (NGF) stimulation. The disruption of this interaction results in aborted NGF-dependent signal transduction critical for neurite outgrowth [10].

**TrkB**: this receptor is specifically activated by the brain-derived neurotrophic factor (BDNF) and neurotrophin 4/5 (NT4/5), after which it interacts with the transmembrane domain of Kidins220 and phosphorylates a specific residue in its cytoplasmic C-terminal tail [2, 10]. In addition, Lopez-Benito et al. have recently shown that Kidins220 negatively regulates the secretion of BDNF [11].

**TrkC**: this receptor is activated upon interaction with NT 3 (neurotrophin 3). Kidins220 does interact with this receptor [10], however, the functional consequences of this interaction are still not described.

Kidins220 also associates with the GluA1 subunit of AMPA receptors through its transmembrane domains, modulating neuronal activity. Decreasing Kidins220 results in a remarkable increase of basal transmission, coupled with alterations in the phosphorylation and surface expression of GluA1-containing AMPAR [12].

#### I.II.3 Poly-proline stretch

This protein-interaction domain is located in the C-terminus of Kidins220 and is known to interact with the adaptor protein CrkL (Crk-like protein) via its SH3 (SRC Homology 3) domain constitutively. Interestingly, upon the Trk receptor-mediated phosphorylation of tyrosine1096 (residue situated within the poly-proline sequence), CrkL binds to Kidins220 through its SH2 domain. This switch in the binding requirement would allow for the release of the SH3 domain of CrkL to recruit C3G and Rap1 and trigger MAPK sustained activation [13]. Peculiarly, Kidins220 is one of the few proteins specifically required for sustained MAPK signalling activation [6], which results in neurite branching. Most of the other elements of the pathway are involved in transient signalling, which entails neurite elongation, as well [14].

#### I.II.4 Sterile-$\alpha$ Motif (SAM)

The SAM domain present in the C-terminal of Kidins220 is one of the most conserved protein interaction domains across species [2]. This domain is arranged in a small five-helix bundle with two large interfaces able to undergo homo- and hetero-

oligomerization as well as polymerization thus forming different types of protein architecture. To date, it is unknown which proteins, if any, interact with Kidins220 by way of SAM.

### I.II.5 Kinesin-Interacting domain (KIM)

The intracellular trafficking of Kidins220 is mediated through a direct binding of KIM to KLC-1 (Kinesin light chain-1) and KLC-2, which are subunits of Kinesin-1. The Kinesin-1 family of molecular motors is implicated in the transport of an increasing number of proteins [15]. KIM overexpression reduces NGF-dependent differentiation of rat pheochromocytoma (PC12) cells, thus suggesting that Kidins220 transport by Kinesin-1 plays a role in the NGF-triggered sustained activation of the MAPK pathway, and subsequent cell differentiation [16].

### I.II.6 PDZ domain

The PDZ domain is a structural domain consisting of 80-90 amino acid residues localized in signalling proteins. PDZ is an acronym combining the first letters of the first three proteins identified to contain this motif (post-synaptic density 95, discs large, zona ocludens-1). The PDZ sequence is instrumental in anchoring various receptors to specific domains of the cell membrane by binding the receptors to the cytoskeleton [17]. By its PDZ-binding sequence, Kidins220 interacts with various proteins:

**$\alpha$-and $\beta$-syntrophin** are scaffold proteins of the sarcolemma of skeletal muscle, at the neuromuscular junction. Syntrophins are diffusely distributed in the sarcolemma during early postnatal stages. Later in development, they become gradually concentrated at the postsynaptic junction sites. $\alpha$-syntrophin plays an important role in the regulation of Kidins220 localization during the neuromuscular junction differentiation. It is likely that $\alpha$-syntrophin works as a scaffold protein for enhancing Eph signalling by recruiting protein complexes to a specific subcellular localization, such as sub-synaptic regions in muscle [18].

**Pdzm3** is a protein involved in early neurogenesis. PDZM 3 and KIDINS220 genes show overlapping expression domains in the hindbrain, ventral retina and motor neurons of zebrafish. The small patch of retinal precursors that express both genes at stage 32 h post-fertilization corresponds to the first post-mitotic cells that differentiate to form ganglion cells with axons extending towards the optic fissure and dendrites branching in the inner retina [19].

**S-SCAM** (synaptic scaffolding molecule) forms a tetrameric complex with Trk receptors, Kidins220 and the Rap1 activator through the PDZ domain present in S-SCAM and the PDZ-binding sequence of Kidins220, to achieve sustained ERK stimulation [15]. The function of N-methyl-D-aspartate receptors (NMDARs) requires the participation of large and dynamic signalling complexes whose formation mainly depends on C-terminal domains, including PDZ-binding motifs present in most NR2 and NR1 (NMDA receptor subunits 1 and 2). Out of the 6 PDZ domains contained in S-SCAM, PDZ5 binds directly to NMDAR subunits, whereas PDZ4 mediates the interaction with Kidins220. Consequently, S- SCAM might also participate in the association of Kidins220 and the NMDARs. Over-activation of NMDARs induces a dramatic downregulation of Kidins220 both in vitro and in vivo. Kidins220 undergoes a comparable regulation in a model of cerebral ischemia, in which NMDARs are over-activated by glutamate pathologically released from neurons in the ischemic core [20].

**SNX27** (sortin nexin 27) is a protein involved in the retrograde transport of endosomes, which specifically binds and directs sorting of PDZ-containing transmembrane proteins, preventing the entry into the lysosomal pathway. This protein interacts with Kidins220 averting the 2-adrenergic receptor degradation during its recycling cycle [21].

p75$^{NTR}$ is a neurotrophin receptor with the potential to dimerize with monomers of any of the three Trk receptors and it interacts with Kidins220 throughout the C-terminal tail. It preferentially binds to proneurotrophins so p75 has the faculty of activating two major pathways [22]:

1. **JNK** (Jun Kinase) signalling pathway: leads to apoptosis through the activation

5 of p53, a cell cycle regulating protein. In neuronal populations, this pathway leads to apoptosis [20].

2. **NF-kB** (Nuclear factor kappa-light-chain enhancer of activated B cells) signalling pathway: promotes neuronal survival [23, 24] by means of the release of the transcription factor NF-kB that leads to the transcription of pro-survival proteins and cytokine production.

A common feature of Kidins220, p75, TrkA and Eph receptors is that they all contain putative C-terminal PDZ-binding motifs. It is, therefore, possible that these proteins are localized to the same subcellular compartment by PDZ domain-containing molecules, and this localization may contribute to signalling events both in development and in adulthood. Kidins220 and p75 expression overlap in adult most notably in the olfactory bulb, Purkinje cells of the cerebellum, and motor neurons of the spinal cord [2].

## I.III Protein interactions with undefined interacting domains

### I.III.1 Protein Kinase-D

Kidins220 owes its name to being the first endogenous substrate of PKD, identified by Iglesias and colleagues [1]. PKD is a serine/threonine kinase distantly related to the PKC family. In cells, DAG (diacylglycerol) and activation of PKC activate PKD [25]. PKD is involved in diverse cellular processes like cell migration, differentiation and polarization [25]. Active PKD is constitutively associated with lipid rafts, which serve as a platform for the signalling cascades triggered by NGF through p75 and TrkA. Activation of these receptors within lipid rafts could result in Kidins220 tyrosine phosphorylation and in signal propagation through this membrane compartment [26].

### I.III.2 Proteins involved in the immune system

T-cell receptor (TCR) and B-Raf interact with Kidins220 promoting sustained Erk activation [26]. Kidins220 interacts with resting and activated B-cell antigen receptor

(BCR) regulating its signalling, which is critical for B-lymphocyte development, proliferation and activation [27].

Kidins220 is an important component of the uropod, the hind part of motile immune cells, where it establishes associations with critical T-cell uropod components. As T-cell polarizes Kidins220, which is initially dispersed on the plasma membrane, becomes highly concentrated at the rear end of the cell, where it co-localizes with proteins normally associated to this structure, such as Intercellular Adhesion Molecule 3 (ICAM-3) and caveolin-1 [28].

Dendritic cells undergo a process of maturation and migration to the lymph nodes where they present antigens to T-cells. The modules and motifs in the cytoplasmic regions of Kidins220 may link this protein to the regulation of the motile processes of dendritic cells and neurons [29].

HIV Tat-induced activation of NF-kB signalling occurs through the interaction between the Inhibitory Kappa B Kinase (IKK) complex and Kidins220 in microglia [30].

### I.III.3 Proteins involved in the cardiovascular system development

Kidins220 constitutively binds to vascular endothelial growth factor receptor (VEGFR) having a key role in angiogenesis. Kidins220$^{-/-}$ embryos display severe cardiovascular deformities, with abnormal heart morphology [31].

### I.III.4 Septin-5

Septins are known to play key roles in supporting cytoskeletal stability, vestibular transport, and endo/exocytosis, stabilizing cellular membranes and forming diffusion barriers [32]. Kidins220 interacts with Septin-5 (CDCrel-1) a member of a highly conserved family of GTP-binding proteins [33]. The role of mammalian septins is not clearly elucidated but it has been reported that Sept-5 inhibits exocytosis by binding to syntaxin 1A [34, 35]. Sept-5 is also accumulated in large amounts at the plasma membrane and at the tips of neurites in NGF-treated PC12 cells [34].

### I.III.5 $Na_v1.2$ channel

Voltage-gated sodium ($Na_v$) channels are responsible for the initiation of action potential at the axonal initial segment. $Na_v$ channels are fundamental players in all kinds of neuronal communications. They are multimeric complexes of $\alpha$ and $\beta$ subunits that exist in several isoforms. The specific channel localization is determined by the interaction of their subunits with a set of adhesion molecules, as well as cytoskeletal and extracellular matrix proteins. There is a higher $Na^+$ conductance in hippocampal Kidins220$^{-/-}$ GABAergic neurons, which might be due to the interaction between Kidins220 and the $Na_v1.2$ subunit. This interaction gains importance in view of the well-established connection between BDNF signalling and neuronal excitability [36].

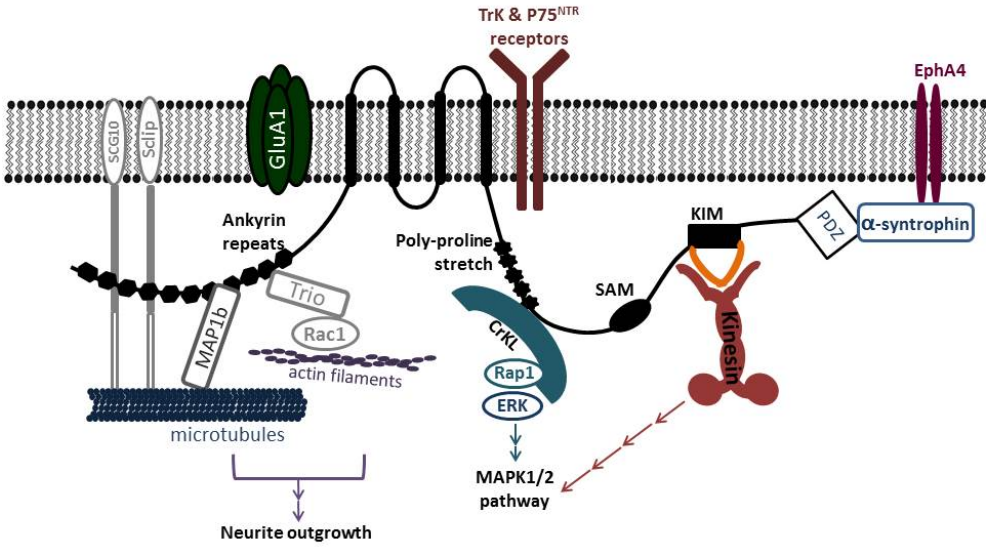


Figure 1. Kidins220 and its interacting proteins. (modified from [37])

## I.IV Kidins220 isoforms

Schmieg and colleagues [38] published a work in which the diverse Kidins220 splice isoforms were described for the first time. In fact the existence of alternative splice isoforms provides an explanation to the diverse functions and localization of this protein in different systems of the organism In total, 6 isoforms were identified in the central region and 3 isoforms at the C-terminal in mice, while 3 isoforms in the central region and 3 at the C-terminal are present in humans (see **Figure 2**). The reduced number of splice isoforms found in humans is due to the fact that exons 27 and 28 are undetectable in the human genome.

Alternative splice isoforms of Kidin220 lacking exons 24-29 are present in adult mouse and human tissues. Because of the severe phenotypes described in the nervous and cardiovascular systems of full Kidins220 KO embryos, which led to embryonic death, the presence of the different isoforms was especially studied in brain, heart and motor neurons. In the mouse brain, isoforms m1, m2, m4, m5 and m6, were recognized. The three human isoforms were detected in brain tissue as well, with a remarkably higher expression of the h3 isoform. Alternative terminal axon (ATE) was also investigated and three alternative endings were discovered: ATE C1, encoding a small portion of exon 32 and exon 33, ATE C2 encoding solely exon 33 and the full legth terminal exon. Cortical and hippocampal cultures were prepared from E18.5 mouse brains. From DIV (days in vitro) 1 to DIV 7 isoforms m4 and m6 were found in all neuronal populations, while from DIV 11 onwards, both populations expressed also isoforms m1 and m3. Interestingly, motor neurons expressed the highest variety of isoforms (all of them with the exception of m2) but lack any significant alternative terminal exon (ATE) splicing. Conversely, ATE C1 and C2 expression increased from E 13.5 until P9. While ATE C1 expression decreased until undetectable levels in adult brain, ATE C2 remained constantly present. The isoform m6/C2 of Kidins220 lacks the KIM, the PDZ and the p75 binding domains. This shorter isoform co-localized with Kidins220 m6 in the cell body seeming to act in a dominant-negative fashion by altering the distribution of the full-length protein. In addition, the isoform m6/C2 was seen to increase the cellular level of TrkA, but

not of p75, while being incapable of forming the ternary complex with TrkA and p75. Considering that an increase in Kidins220 full length expression leads to a decrease in the interaction between TrkA and p75, it was proposed that the fine-tuning of neurotrophin signalling function could be achieved by varying the levels of the different ATE isoforms. Furthermore, the fast appearance of isoform m1 upon BDNF stimulation in cortical and hippocampal neurons suggests that neurotrophins might influence Kidins220 function by controlling the expression of its multiple isoforms [39].

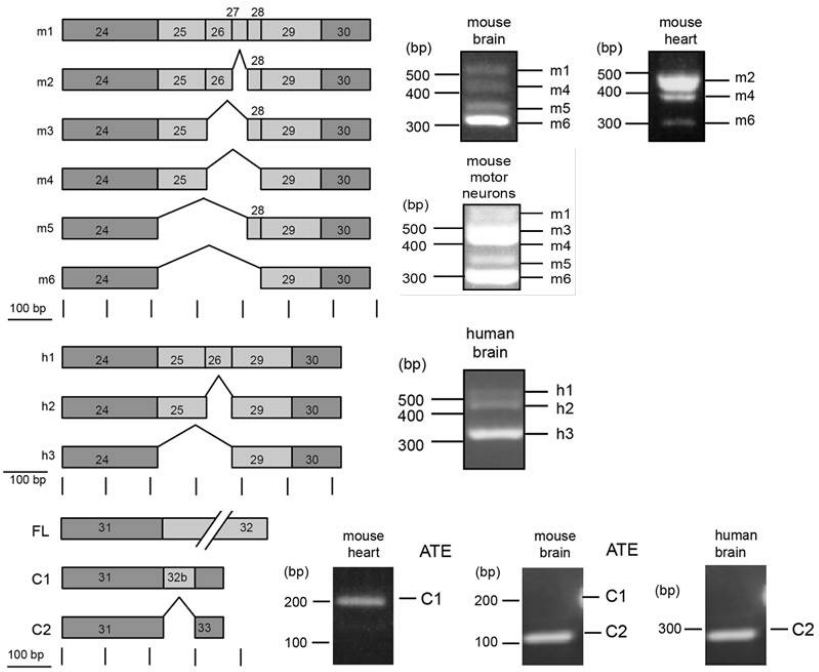


Figure 2. Schematic representation of Kidins220 alternatively spliced isoforms [38]. The first 6 isoforms in the upper part are found in mouse tissue (m), while the subsequent three are found in human tissue (h). At the bottom the splicing isoforms of the carboxy terminal, present in mouse and human, are represented. On the right, representative PCR products for the isoforms detected in different adult mouse and human tissues.

## I.V Kidins220 and diseases

### I.V.1 Tumour development

Kidins220 protein overexpression has been related to a wide array of cancers (for review see [40]). The overexpression of Kidins220 was found to facilitate **melanoma** formation by suppressing MAPK-mediated stress-induced cell death, and it correlated with reduced patients survival [41].

Kidins220 is also involved in the development of neuroblastoma, a tumour originating from the neural crest. Kidins220 promotes the survival of neuroblastoma cell lines by mediating NGF-induced MAPK signalling [42]. Accordingly, the knockdown of Kidins220 inhibited cell proliferation relenting the G1 phase of the cell cycle [43]. Thus Kidins220 was identified as a possible target for neuroblastoma treatment [44]. Among others, genetic screening described an intragenic break point in the human KIDINS220 gene related to paediatric high-grade **glioma** (pHGG) [45].

### I.V.2 Alzheimer's disease

Increased expression of Kidins220 is also associated with the development of Alzheimer's disease (AD). AD is characterized by three main pathophysiological characteristics: extracellular senile plaques containing (A$\beta$) and intracellular neurofibrillary tangles (NFT) and hyper-phosphorylated forms of the microtubule-associated protein (MAP) Tau [46]. The accumulation of Kidins220 in AD was strongly associated with the accumulation of Tau [47]. Since under physiological conditions Kidins220 is cleaved by calpain upon neuronal excitotoxicity [20], it was proposed that GSK3-mediated phosphorylation of Kidins220 in the AD brain would protect it from the cleavage. Moreover, the quantification of the N-terminal of Kidins220 in the cerebrospinal fluid of AD patients has been proposed as a biomarker for this disease [48].

## I.VI Autism Spectrum Disorder

Autism Spectrum Disorders (ASD) are characterized by two key diagnostic elements [49]: persistent deficits in social communication (verbal and non-verbal) and social

interaction across multiple contexts and restricted, repetitive patterns of behaviour, interests, or activities.

Several studies have related Kidins220 with ASD. Increased expression of Kidins220 (2.16-fold change) was detected in the blood transcriptome performed on 170 ASD patients and 115 controls. Kidins220 gene was one of the 12 genes with an average fold change bigger than 1.5. Moreover, alteration of the neurotrophin signalling pathways is known to be enriched in ASD patients, including the MAPK, phosphatidylinositol 3-kinase (PI3K) and phospholipase-C (PLC) pathway. These pathways not only are key to neuronal development and plasticity, learning and memory but also involve Kidins220 [50]. A genetic screening also related Kidins220 with ASD, identifying heterozygous deletions of the gene in 3 out of 2446 families [51].

One of the most intriguing aspects regarding the genetics of ASD is the elevated number of genes found to be associated with this disorder and the convergence of these genetic risk factors to the same general cluster of symptoms diagnosed as ASD. It is believed that this is due to the fact that ASD development depends on convergent downstream mechanisms, which can be affected by diverse genetic variants. In line with the diversity of risk factors, there is a high heterogeneity in the symptomatology of ASD across patients [52]. This is why the research of this psychiatric disorder involving animal models is focusing on the distinguishable subgroups of biological defects known to be present in groups of ASD patients, known as endophenotypes. As genetic mouse models have emerged in the ASD research, behavioural assays with high relevance to the diagnostic symptoms of autism have been developed. Considering the types of social deficits in communication and interaction common in ASD, social behaviour tests have been developed such as the 3-chamber test [53], social interaction test, social memory test, olfactory habituation test [54]. Moreover, call categories for responses to social vocalizations, emitted in response to social cues during reciprocal social interactions, have been described [55]. For the evaluation of repetitive behaviours and motor stereotypes, behavioural tests relevant to anxiety, cognitive impairment, hyperactivity and sensory reactivity are used [52], including the open field, elevated plus maze, light-dark, fear conditioning, Y maze, and Morris water maze tests, as well as the quantification

of grooming behaviour.

Considering the connection between Kidins220 and ASD, the aforementioned behavioural parameters have been tested during this project by performing some of these tests on Kidins220 mutant animals.

## I.VII Schizophrenia

Schizophrenia is a dynamically evolving, neurodevelopmental psychiatric disorder best understood from the psychobiological perspective [56]. Thus, regarding heritability, genetic and epigenetic variants are both crucial risk factors to be considered when diagnosing this disorder.

Kidins220 has been related to schizophrenia via genetic studies. In 2015 Kranz and colleagues, performed a targeted exome capture of selected neurotrophin genes, including the Trk receptors, p75, the four main neurotrophins and the Trk interactors Kidins220 and TRIO [57]. Out of 48 cases, 5 were carriers of variations in the KIDINS220 gene, identified as 2 rare missense polymorphisms and 1 novel missense mutation. One of the two polymorphisms was located between transmembrane (TM) domain 2 and TM3, and the other within the SAM domain. As previously mentioned, TM domains mediate the interaction between Kidins220 and multiple receptors, i.e. AMPAR, Trk and p75NTR, while the SAM mediates protein-protein interactions. The novel missense mutation was located in the poly-proline stretch, the region that interacts with CrKL leading to sustained MAPK activation (see **Figure 3**), and the patient carrying such mutation had severe symptomatology. It is still not known to what extent these sequence variations affect the physiological interactions of Kidins220 and the downstream pathways. Moreover, 50% of the identified missense coding variants were found in the NGF-TrkA-Kidins220 pathway. Another study involving 22 schizophrenia patients and 11 controls investigated the association between the rostralization ratio of N- acetyl-L-aspartate (NAA), which is a neuronal-specific metabolite that indicates neuronal health and integrity, with rare missense polymorphisms in PTPRG, SLC39A13, TGM5, NTrk1 and KIDINS220. This study showed that deficient rostralization is significantly correlated with ver-

bal decrements and with trait-negative symptoms in schizophrenia. KIDINS220 and NTrk1 gene variants were located in functional protein domains as the SAM and the transmembrane domain (see **Figure 3**) [58]. Another study reported the phenotypes of subsets of cases with missense coding polymorphisms or novel mutations in four different genes: PTPRG, SLC39A13, TGM5, KIDINS220, considered genes potentially relevant for psychosis. Remarkably, KIDINS220 missense carriers had lower mean verbal and full-scale IQ scores, and more severe general psychopathology symptoms than the other groups. In addition, KIDINS220 variant carriers experienced a severe form of degenerative joint disease. KIDINS220 missense carriers demonstrated the second slowest processing speed but they scored similarly on all cognitive measures [59].

A significant overlap of biological pathways between ASD and schizophrenia has been established by various studies [60]. Among these common pathways, the small GTPase family (including subfamilies if the Ras, Rho, Arf, Ran and Rab GTPases [61]) and MAPK signalling are particularly relevant as they contain many genes associated to neurodevelopmental disorders, and have been implicated in synapse plasticity and behaviour [62]. Given the scaffolding function of Kidins220, we hypothesize that it may represent an element of convergence of signalling pathways whose alterations are shared between these two disorders.

## I.VIII SINO syndrome

SINO is an acronym for a symptomatology characterized by spastic paraplegia, intellectual disability, nystagmus and obesity, described in three unrelated pediatric (between 1 and 3 years old) patients carrying *de novo* nonsense variants in the KIDINS220 gene [63]. This *de novo* variants resulted in truncated isoforms of the Kidins220 protein similar to the ATE C2 splicing variant previously described (see **Figure 4**) [38], which is mainly expressed during adulthood. This indicates that the disruption of the Kidins220 isoforms repertoire possibly caused the neurological phenotype found in these patients. As shown in **Figure 4**, the C-terminal region of Kidins220 contains the KIM and PDZ domains, which are crucial for protein in-

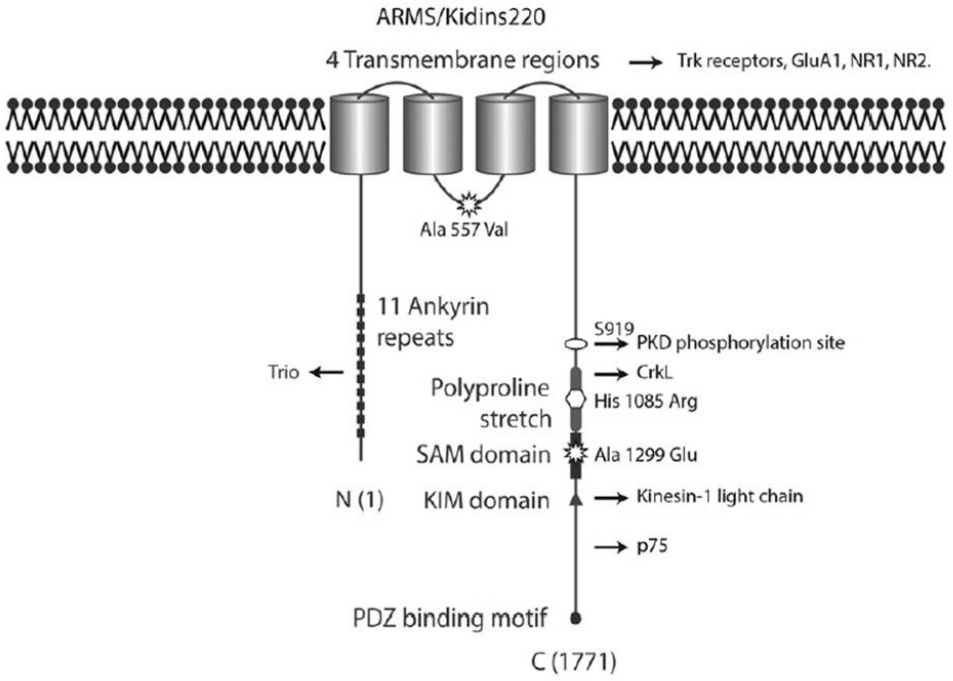


Figure 3. Schematic representation of the location of missense variations and mutations in Kidins220 correlated with schizophrenia [57].

teractions and transport, as explained in paragraph I.I.1.5.KIM domain, I.I.1.6.PDZ domain. the expression of KIDINS220 is developmentally regulated and differential splicing occurs in specific tissues as brain, heart and skeletal muscle. Motor neurons exhibit the highest variety of alternative splicing in the middle region, but do not express ATE splicing. So these patients' variants resemble isoforms that are not normally expressed in the developing embryo or present in motor neurons. Indeed the motor symptoms showed by these patients, i.e. spastic paraplegia and nystagmus, might be explained by the abnormal expression of the full-length isoform in motor neurons. The pathophysiology of obesity is instead more probably related to the involvement of Kidins220 in neurotrophin signalling, since neurotrophins, and especially BDNF, have been largely related to the control of body weight [64]. Remarkably, the three patients showed dilated lateral and third brain ventricles, strongly

reminiscent of the phenotype obtained from Kidins220$^{-/-}$ and cKO mice [31], Satapathy & Almacellas, (*Manuscript in preparation*: see paragraph I.II.1.Kidins220 KO line; I.II.3.Kidins220 cKO line). However, not every loss-of-function variant in the last exon of KIDINS220 causes the phenotype observed in the patients described here, as three different variants have been identified in 5 healthy individuals [63].

One year after Josifova's et al. work was published, a frameshift variant in exon 24 of the KIDINS220 gene was identified by Mero and colleagues. This variant was the cause of a severe and progressive hydrocephalus, and extensive limb contractures at gestational week 18, which lead to 4 abortions in a consanguineous couple [65]. These fetuses showed very similar phenotypes to those seen in Kidins220$^{-/-}$ embryos and in the three above-described patients, proving the key role Kidins220 has in the healthy embryonic development in humans.

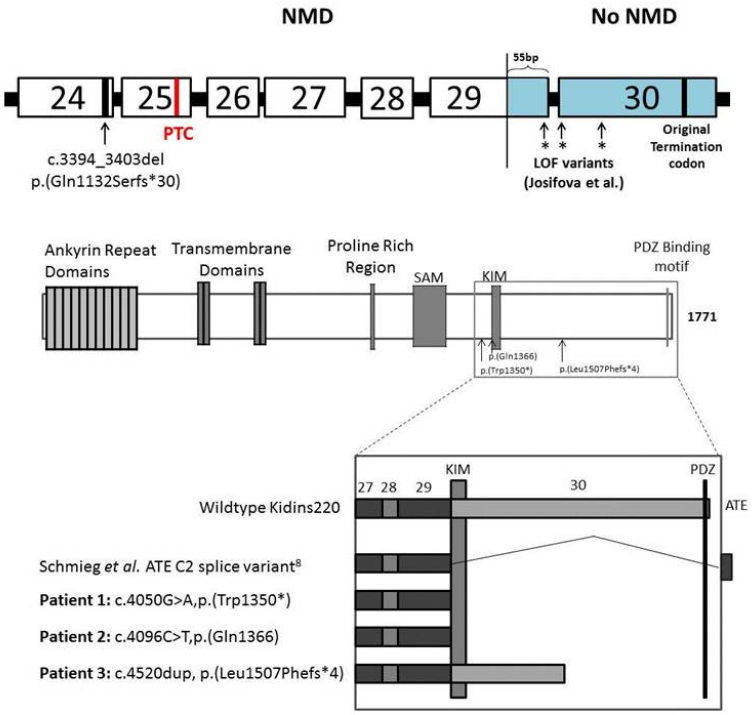


Figure 4. Schematic representation of the de novo variants described in the papers [63, 65]. **Above:** figure modified from [65]. PTC=premature termination codon, which would be predicted to elicit nonsense-mediated mRNA decay (NMD). The blue-colored area is predicted to escape NMD. **Bottom:** Figure from [63] with the loss of function (LoF) variants described in the article

## I.IX Kidins220 transgenic lines

Two complete knockout (KO) mouse lines of Kidins220 have been developed, which are both not viable beyond the embryonic period.

### I.IX.1 Kidins220 KO mouse line

The full Kidins220 KO mouse line was generated in Dr Schiavo's laboratory and first described in 2011 [66]. It was generated by inserting a Kidins220 cDNA-polyA cassette flanked by two floxP sites in the unique *Nrul* site of the Kidins220 gene. Kidins220$^{lox/lox}$ mice were crossed with animals expressing Cre recombinase under the phosphoglycerate kinase (PGK) promoter to enable Cre activation since embryogenesis [67]. Thus, a mouse line was generated on the C57Bl6/J background, in which the KIDINS220 gene was ablated from the early embryonic stages. Mice bearing the deletion in the germline were subsequently crossed, originating heterozygous (Kidins220$^{+/-}$) animals ubiquitously lacking one Kidins220 allele.

Kidins220$^{+/-}$ animals were viable and fertile. They expressed the same amount of protein as WT mice and did not show any overt behavioural phenotype. However, no Kidins220$^{-/-}$ mice were present in the offspring of Het x Het matings, suggesting that the early homozygous ablation of the KIDINS220 gene was lethal. Indeed it was seen that up until E15 all embryos were comparable, however by E18 the Kidins220$^{-/-}$ embryos displayed severe growth defects (**Figure 5**). The brains were notably smaller when compared with Kidins220$^{+/+}$ littermates and their hearts showed dilated and congested atria as well as disorganized ventricular walls. These severe heart deformities lead to the identification of the interaction between Kidins220 and VEGFR, which is key for cardiovascular system development, as previously described. Kidins220 KO embryos exhibited extensive cell death in both the central and the peripheral nervous system, in line with the neuronal loss seen in the fetuses studied in the paper from Mero and colleagues [65]. Moreover, Kidins220$^{-/-}$ primary neurons displayed an impaired response to BDNF, leading to deficiencies in cell survival, axonal/dendritic differentiation as well as in the BDNF-induced potentiation of EPSCs [31, 66].

The interaction between Kidins220 and $Na_v1.2$ was studied using cultures of primary neurons derived from Kidins220 KO embryos. This project led to the characterization of the properties of excitatory and inhibitory neurons lacking Kidins220, which included hyperexcitability and faster recovery of GABAergic neurons from trains of stimuli. The KO mouse line has been also used for the study of KO astroglia. KO astrocytes show impaired survival/death pathways, specifically reduced death pathway activation upon ultraviolet radiation and reduced phosphorylation of MAPK upon BDNF stimulation. Moreover, WT neurons in mixed culture with KO glia show reduced frequency and firing threshold compared to WT neurons grown with WT glia (Jaudon et al., *manuscript in preparation*).

### I.IX.2 ARMS heterozigous mouse line

Another line of Kidins220 KO mice was generated in Dr Chao's laboratory in 2009, which will be referred to as ARMS KO to avoid confusion with the strain described in paragraph I.IX.1. This line was generated using the Cre/lox system, by crossing ARMSlox mice with animals bearing Cre under the actin promoter, which is ubiquitously expressed and active from embryogenesis [68]. The ablation of Kidins220 was lethal at an early embryonic stage also in this mouse model. However, $ARMS^{+/-}$ mice were viable and expressed approximately 70% of the physiological amount of the protein. They displayed decreased dendritic complexity and reduced spine stability [4], and moreover, $ARMS^{+/-}$ female mice showed reduced spatial memory formation coupled with cell death in the frontal and entorhinal cortex [69].

### I.IX.3 Kidins220 conditional KO (cKO) lines

The biggest challenge in the study of the function of Kidins220 is to discern how this protein affects the functioning of the adult brain. That is why a cKO line was generated by crossing $Kidins220^{lox/lox}$ mice with animals expressing Cre under the nestin promoter, obtaining the nervous system-specific ablation of Kidins220. Nestin- cKO animals were born alive, however, they died soon after birth due to a neurological impairment leading to impaired suckling behaviour, and were not further analyzed [66].

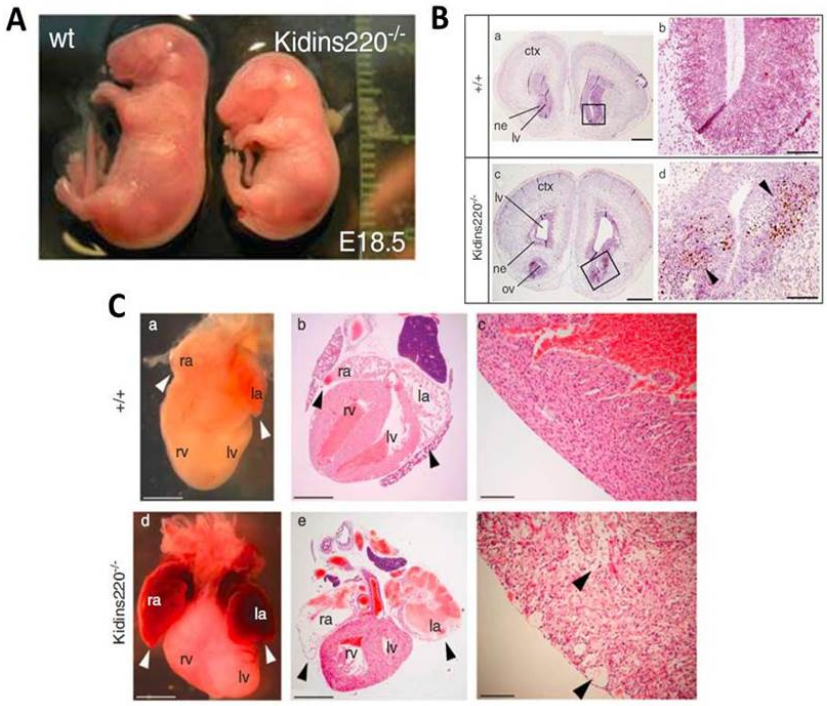


Figure 5. Main phenotypes of the Kidins220$^{-/-}$ mouse line. **A.** Picture of Kidins220$^{+/+}$ and Kidins220$^{-/-}$ (KO) E18.5 embryos, where the difference in size can be appreciated. **B.** Picture of brains from WT and KO mice where the difference in size can be also seen. **C.** Heart deficits in Kidins220$^{-/-}$ embryonic heart. Kidins220 KO hearts show congested atria and higher magnification of the right ventricle wall. [31, 66]

Another cKO line was then generated in Dr Cesca's laboratory, using the same recombinase system, but this time expressing Cre under the Calmodulin-Kinase II (CamKII) promoter, which led to the ablation of Kidins220 in the excitatory neurons of the forebrain, starting from the second postnatal week (**Figure 6**). The data shown in this and the following paragraphs were obtained by Dr Satapathy and Dr Jaudon and represent the basis of the original work described in this thesis. The forebrain-specific deletion of the protein was validated by western blot analysis (**Figure 6 B**). Biochemical analysis performed on WT and cKO brains showed reduced basal levels of phosphorylated TrkB and phosphorylated MAPK (**Figure 6 C**). This line was established as a tool for investigating the role of Kidins220 in the development and functioning of cortico-hippocampal circuits, and in the establishment of higher cogni-

tive functions and social skills.

Kidins220 cKO (lox/lox; +/CaMKIICre) mice showed comparable development to their WT (+/+; +/Cre) littermates regarding body weight, size and appearance. A closer analysis of the brain revealed no cell death in the hippocampus and cortex, no alterations of the cortical layers and no gross defects of myelination (data not shown). Dendritic arborization was quantified in the motor and sensory cortex, revealing a decreased complexity of neurons of the motor cortex in cKO animals (**Figure 7**).

For a more comprehensive study of the involvement of Kidins220 in the functioning of the adult brain, a behavioural characterization of the CaMKII-Cre Kidins220 cKO mouse model was performed. Before starting with the behavioural testing it was necessary to validate the general health condition of the cKO animals through a battery of tests to check the general health, neurological reflexes, home cage behaviours and sensory-motor functions. This analysis did not reveal any behavioural alteration of cKO animals (**Figure 8 A**). As previously mentioned, a great variety of behavioural tests have been validated for the study of cognitive functions as memory, anxiety, risk-taking etc. Because of the engagement of Kidins220 in neurotrophin signalling and the connection between BDNF and anxiety and memory [70], the mice were challenged in the open field, Y maze, light-dark and Morris water maze tests. The open field test is based on the fear of mice to open spaces and it consists on monitoring the free movement of the mice in a cage for one hour. This test allows quantifying anxiety and hyperactivity. cKO mice showed a burst of hyperactivity when first introduced in the novel arena, and a constant higher presence in the central zone compared to the WT, indicating a low-anxiety phenotype (**Figure 8 B**). The Morris water maze tests spatial memory by training the animals to find a platform in a determinate quadrant of a pool filled with opaque water. After 5 training days, the ability of animals to remember the position of the platform is evaluated. The spatial memory is extrapolated by the amount of time the mice spent in the correct quadrant. cKO females showed impaired spatial memory in the test trial, in line with the results shown previously with the ARMS$^{+/-}$ mouse line [69] (**Figure 8 C**). No genotype differences were found in the Y maze test, which measures short-term spatial memory, and in the light-dark test, which evaluates anxiety (not shown).

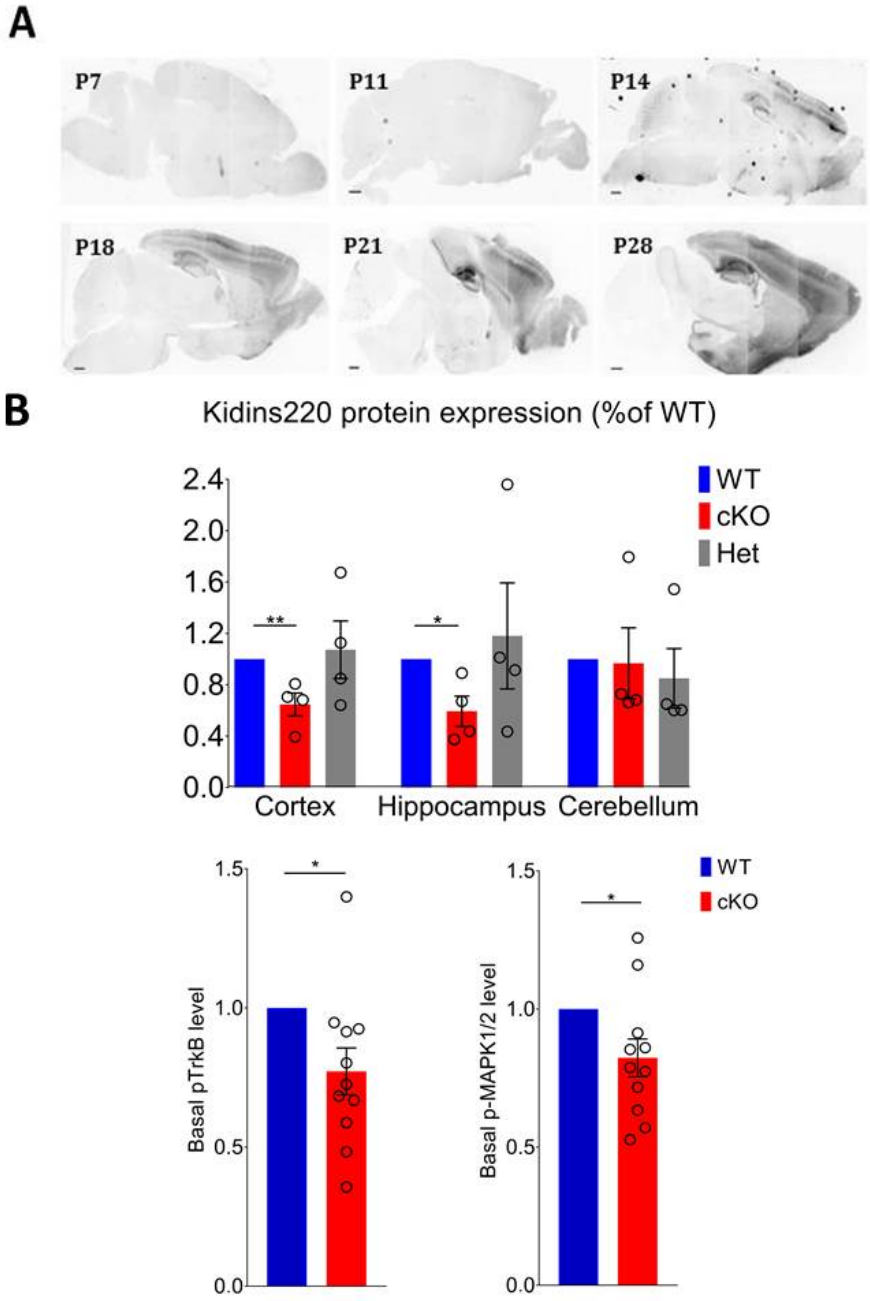


Figure 6. **CaMKII-driven cKO mouse line validation A.** Sagittal brain slices were obtained from the offspring of CaMKIICre mice crossed with dt-tomato$^{lox/lox}$ animals, at different post-natal stages. The fluorescence identifies the brain regions where Cre is active. **B. (Above)** Protein quantification from western blotting assays of brain lysates of 2-month old WT, Het and cKO mice. Kidins220 expression is significantly low in the cortex and hippocampus of Kidins220 cKO mice than in WT animals, while the expression is comparable between the two genotypes in the cerebellum, as expected (One-way ANOVA, followed by Bonferroni's *post-hoc* test $**p < 0.01; *p < 0.05$; n=4 animals per genotype). **(Below)** Protein quantification of phosphorylated MAPK and TrkB from lysed brain slices ( $*p < 0.05$ Students t-test, n=10 slices per genotype) (Satapathy, Almacellas-Barbanoj et al., *manuscript in preparation*).

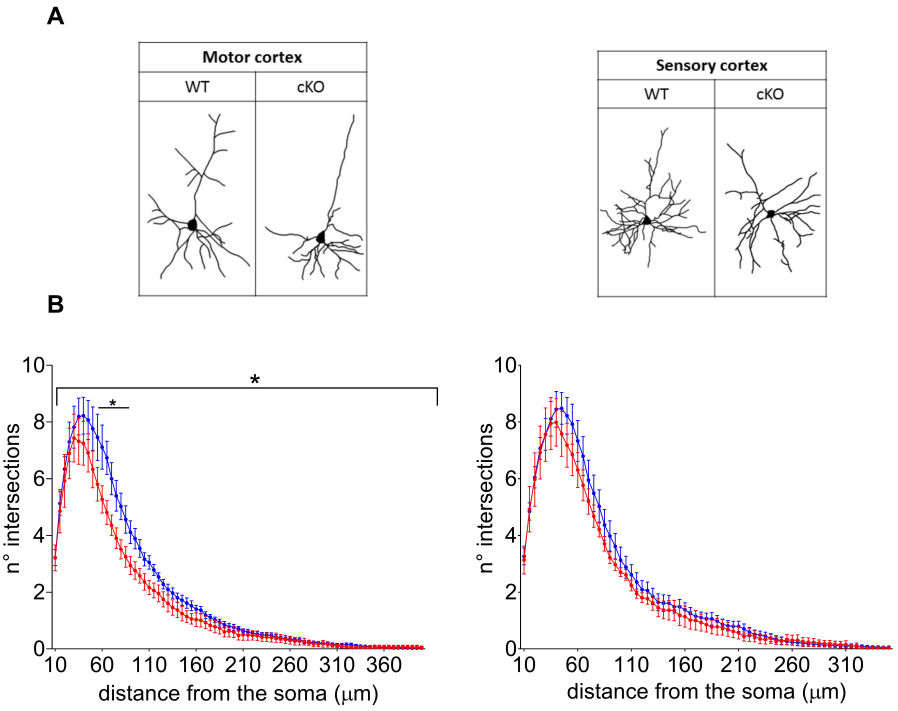


Figure 7. **Sholl analysis of neurons of the motor and sensory cortex of cKO and WT mice.** Representative images **(A)** and Sholl analysis **(B)** of neurons from the motor and sensory cortex of 2-3 months old cKO and WT mice, Brains were stained by the Golgi-Cox methods, subsequently sliced and imaged. WT (blue) n=6 animals cKO (red) n=6 animals. The Sholl analysis in the motor neurons showed a significant genotype effect ($F_{1,10} = 5.248, *p < 0.05$, RM-ANOVA, Sidak's multiple comparisons post-hoc test indicates significantly less intersections in Kidins220 cKO neurons at radius 55-70 $\mu$m ) (Satapathy, Almacellas-Barbanoj et al., *manuscript in preparation*).

A

| | WT n=8 | cKO n=8 |
|---|---|---|
| **Appearance** | | |
| Poor Coat Condition (%) | 0 | 0 |
| Bald Patches (%) | 0 | 0 |
| Missing Whiskers (%) | 0 | 0 |
| Piloerection (%) | 0 | 0 |
| Abnormal Response (%) | 0 | 0 |
| **Motor Functions** | | |
| Trunk Curl (%) | 100 | 100 |
| Forepaw Reaching (%) | 100 | 100 |
| Co-ordiation and Balance on Beam (3 point scale) | 2±0 | 2±0 |
| Grip Strength ( 3 point scale) | 2±0 | 2±0 |
| **Reflexes** | | |
| Righting Reflex (%) | 100 | 100 |
| Eye Twitch (%) | 100 | 100 |
| Ear Twiych (%) | 100 | 100 |
| Whisker Orientating Reflex (%) | 100 | 100 |
| Postural Reflex (%) | 100 | 100 |
| **Sensory Functions** | | |
| Visual Placing (%) | 100 | 100 |
| Negative Geotaxis (%) | 100 | 100 |
| Acoustic Startle Response (%) | 100 | 100 |
| **Analgesic Behaviour** | | |
| Hot Plate Latency (seconds) | 145±12 | 127±15 |

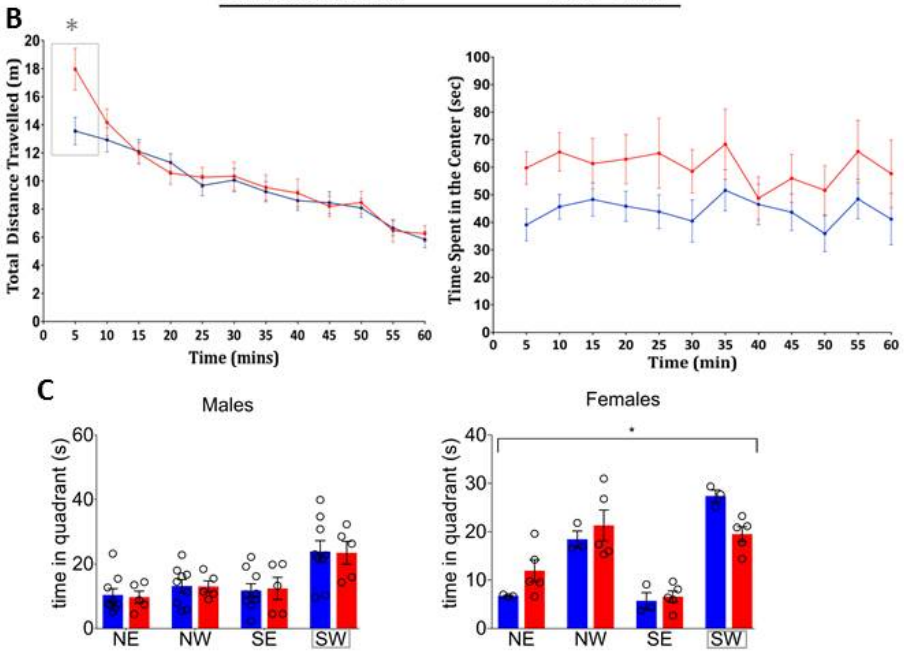


Figure 8. **A**. A battery of health tests showed the comparable motor and sensory function and appearance of WT and cKO mice. **B**. Results of the open field test. **Left:** total distance travelled during the 60 min test. The grey rectangle indicates higher locomotor activity by the cKO mice during the first 5 minutes (Student's t-test, $*p < 0.05$) **Right:** time spent in the central zone. WT (blue) n=21 cKO (red) n=18 cKO mice spend significantly more time in the centre throughout the entire test with a significant genotype effect ($F_{1,37} = 4.568, *p < 0.05$, RM-ANOVA). **C**. Morris water maze test results, depicted as the amount of time spent in each quadrant of the maze. The south-west quadrant was the one where the platform was located during the training. WT (blue)= 9 males and 3 females; cKO (red)= 5 males and 5 females. Males from both genotypes showed the expected performance during the test with a significant trial effect indicated in the graph ($F_{3,48} = 9.9, * * * * p < 0.001$, RM-ANOVA ). Kidins220 cKO females showed globally poorer performance. Statistical analysis revealed a signifficant effect, not indicated in the graph for clarity ($F_{3,24} = 28.95, * * * * p < 0.0001$, RM-ANOVA) with a significant genotype-trial interaction, indicated in the graph ($F_{3,24} = 3.45, *p < 0.05$, RM-ANOVA) and significant trial effect indicating different amount of time in each quadrant, not indicated in the graph for clarity (Satapathy, Almacellas-Barbanoj et al.,*manuscript in preparation*).

## I.X Aim of the study

A growing amount of literature has identified Kidins220 as a risk factor for important psychiatric diseases such as autism spectrum disorders and schizophrenia. Moreover, mutations in the KIDINS220 gene have been recently identified, which cause severe neurological phenotypes in human patients. The scaffolding function of this protein makes it a key convergence factor of crucial signalling pathways, and a promising element to gain further knowledge on the endophenotypes of these developmental disorders, and their molecular basis. Given the embryonal/early postnatal lethality of the full and nervous system-specific Kidins220 knockout animals, the development of the CaMKII-Cre cKO model represents an extremely useful tool for discerning the role of Kidins220 in the functioning of the adult brain, and the alterations caused by the lack of this protein. On the basis of these considerations, the aim of this project is to complete the behavioural characterization of the CaMKII-Cre mouse line using as a guideline the characteristic symptomatology of ASD and schizophrenia-like mouse models. Importantly, the same characterization is performed on the Kidins220$^{lox/lox}$ ; Kidins220$^{+/+}$ mice. This is mandatory given the crucial, and only recently appreciated role of alternatively spliced Kidins220 isoforms in central nervous system physiology. This approach will allow us to discriminate and understand the contribution of Kidins220 isoforms (or the lack of thereof) in the pathogenesis of disorders affecting cognition and the social sphere.

# II Results

## II.I Rationale of behavioural assessment

The main advantage of the cKO model for Kidins220 is its viability, which allowed us to address the role of Kidins220 in various behavioural paradigms in adult mice. On the basis of the known roles of Kidins220 described in the literature (see Introduction), we focused on the following aspects of adult behaviour:

1. Learning and memory (Morris water maze, fear conditioning);
2. Anxiety (open field, elevated plus maze);
3. Social skills (social habituation / dis-habituation, social memory and olfactory abilities);
4. Sensory-motor gating (pre-pulse inhibition and startle response).

With the exception of the Morris water maze, which was entirely performed by Dr Satapathy, in this thesis, I describe all the experiments that I contributed to either partially (anxiety experiments and fear conditioning) or completely (social experiments and sensory gating tests).

All experiments were performed with age-matched, littermate animals. Males and females were analysed separately in all the experiments. If sex-specific phenotypes were observed, results from the two genders were shown separately; otherwise, they were pooled together. The cKO and Kidins220$^{lox/lox}$ animals were obtained through the mating scheme described in Materials and Methods (see **Figure 19**), and the tested animals were of the following genotype:

1. WT (Cre/+; +/+), blue colour in all figures, vs cKO (Cre/+; lox/lox), red colour;
2. Kidins220$^{+/+}$ (+/+; +/+), cyan colour, vs Kidins220$^{lox/lox}$ (+/+; lox/lox), orange colour.

### II.I.1 Fear conditioning

The protocol we followed to assess conditioned fear and contextual memory is shown in **Figure 9 A** and detailed in the 'materials and methods' section. Briefly, the conditioned fear is generated by pairing a footshock with an acoustic cue. 24h later the fear paired to the context and the cue (associative learning) is tested. Data for the cKO line are shown in **Figure 9 B**, while data for the Kidins220$^{lox/lox}$ line are shown in **Figure 18**. The strength of the association between the context and cue and the foot-shock is reflected in the amount of time the mice freeze. During the '*fear conditioning*' (**Figure 9 B, C, left**) the freezing behaviour increased as more trials (cue + foot-shock) were performed, showing a comparable trend in all genotypes. In the '*context*' phase (**Figure 9 B, C, middle**), which took place 24 h later, cKO females froze significantly less than their WT littermates. Importantly, we did not see this difference between cKO and WT males, in line with the water maze results (see **Figure 8**, Introduction). On the other hand, in this phase of the test the performance of Kidins220$^{lox/lox}$ animals was comparable to Kidins220$^{+/+}$ for both sexes. In the '*novel context + cue*'phase(**Figure 9 B, right**), performed 1 h later, cKO mice displayed normal freezing behaviour in response to the auditory cue, while Kidins220$^{lox/lox}$ mice froze significantly more than Kidins220$^{+/+}$ animals. As disussed in section III.III, WT and Kidins220$^{+/+}$ animals display different freezing behaviour during the '*novel context + cue*'phase and will be further discussed in the mentioned parahraph.

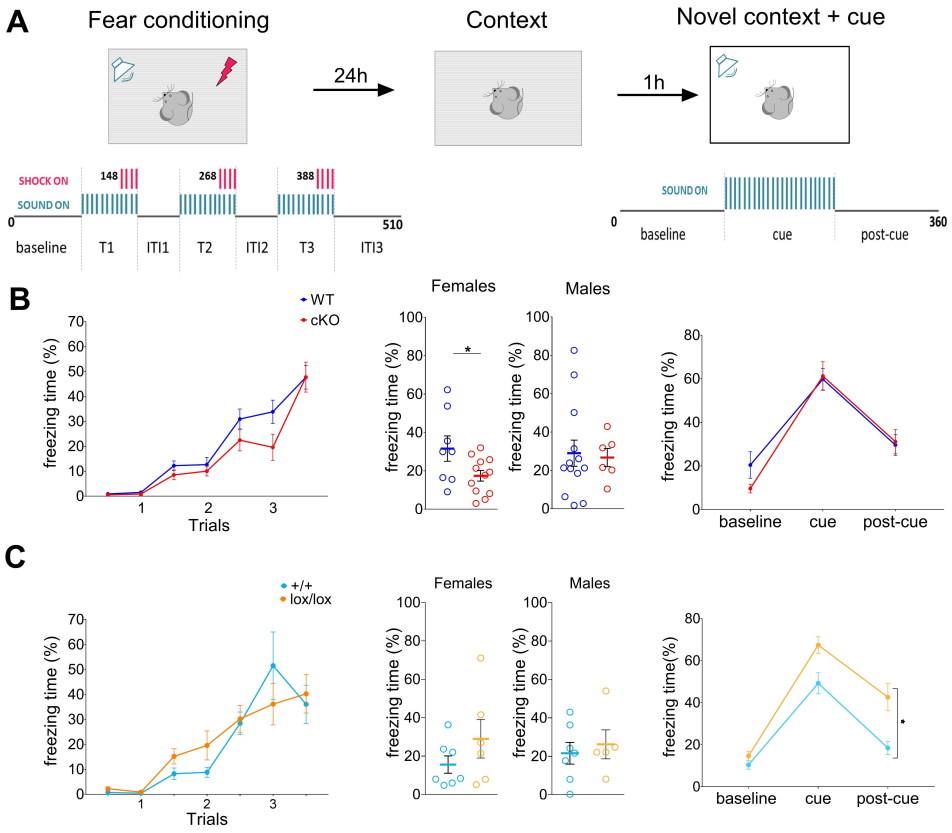


Figure 9. **Fear Conditioning. A.** The three phases of the experiment are shown: the '*fear conditioning*', the '*context*' and the '*novel context + cue*' phase. The timeline of the shock and auditory cues is shown below. In B and C, the amount of time the mice spent freezing during each phase of the experiment is shown as % freezing time. **B.** Results for WT (n = 22, blue) and cKO (n = 17, red) mice. **Left:** % freezing time for the 3 trials of the '*fear conditioning*' phase. The animals spent significantly more time freezing as the conditioning trial progressed (trial effect: $F_{6,210} = 57.89, ****p < 0.0001$ repeated measures (RM) ANOVA), as expected. Both genotypes show comparable freezing behaviour (genotype effect: $F_{1,35} = 2.81$ repeated measures (RM) ANOVA) **Middle**: The % freezing time during the '*context*' phase is shown separately for males and for females, each circle representing one individual. cKO females froze significantly less than WT females ($*p < 0.05$, Student's t-test), while no difference was observed for males. **Right**: no genotype effect is found in the '*novel context + cue*' trial, where cKO animals show a conditioned behaviour comparable to WT Indeed, mice of both genotypes showed an effective and comparable conditioning to the cue (genotype effect: $F_{1,37} = 0.218$ repeated measures (RM) ANOVA), as determined by increased freezing behaviour (trial effect: $F_{2,74} = 62.96, ****p < 0.0001$ RM-ANOVA). **C.** Results for Kidins220$^{+/+}$ (n = 13, cyan) and Kidins220$^{lox/lox}$ (n = 11, orange) mice. The behaviour of Kidins220$^{lox/lox}$ mice was comparable to Kidins220$^{+/+}$ animals in both the '*fear conditioning*' (genotype effect: $F_{1,23} = 0.112$ repeated measures (RM) ANOVA) (**Left**) and the '*context*' (**Middle**) phase. The conditioning protocol was effective (trial effect: $F_{6,138} = 19.53, ****p < 0.0001$ RM-ANOVA). The time freezing (%) during the 'context' trial was comparable between Kidins220$^{lox/lox}$ and Kidins220$^{+/+}$ in males and females ($p > 0.05$; Student's t-test). **Right**: mice of both genotypes showed an effective conditioning to the cue, as determined by increased freezing behaviour (trial effect: $F_{2,42} = 83.66, ****p < 0.0001$ RM-ANOVA), however Kidins220$^{lox/lox}$ animals showed increased freezing, when compared to Kidins220$^{+/+}$ mice (genotype effect: $F_{2,42} = 4.1, *p < 0.05$ RM-ANOVA, indicated in the graph; Sidak's multiple comparisons *post-hoc* test $**p < 0.01$ in '*cue*', $***p < 0.001$ in '*post-cue*' not indicated in the graph for clarity). Data are represented as mean  s.e.m. in all panels.

### II.I.2 Elevated plus maze

The 'elevated plus maze' test (**Figure 10 A**) is a commonly used protocol to test anxiety levels in rodents. It is based on the principle that open spaces elicit anxiety on mice. The level of anxiety in the mice is extrapolated by the amount of time the animals spend in the open arms, whereby a high level of anxiety will be reflected on a reduced amount of time spent in the open arms. This test was partly done by Dr Satapathy. cKO mice entered more times to the open arms, compared to the WT mice (**Figure 2 B**). However, mice of both genotypes spent a comparable amount of time in the open arms. Kidins220$^{lox/lox}$ animals instead behaved similar to Kidins220$^{+/+}$ mice in terms of both the number of entrances in the open arms, and time spent there (**Figure 10 C**).

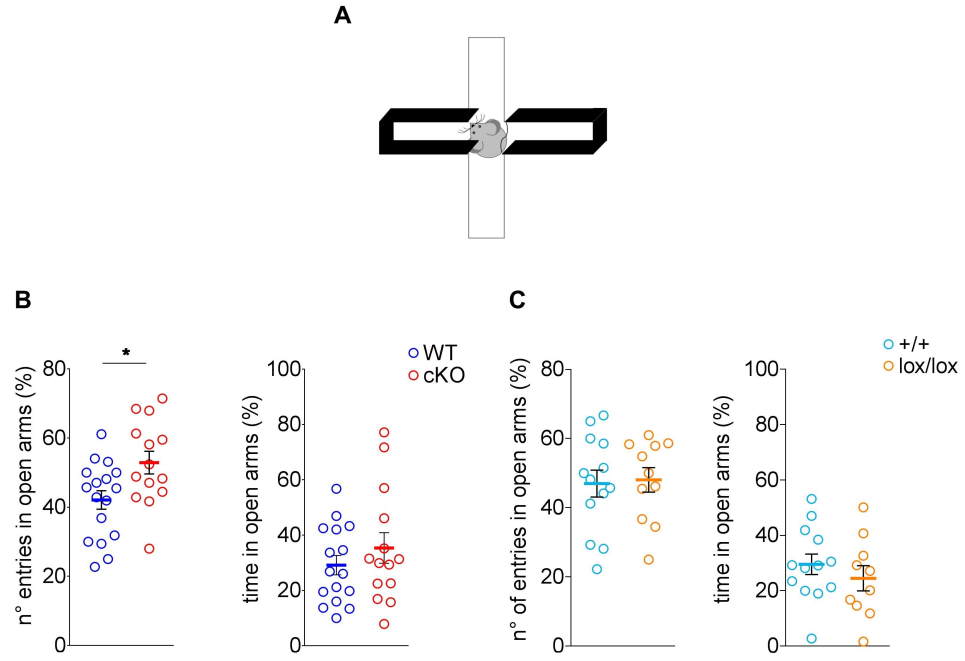


Figure 10. **Elevated Plus Maze A.** Schematic representation of the maze, with 2 open arms and 2 closed arms. **B.** Results for WT (n = 17, blue) and cKO (n = 14, red) mice. Bar graphs (each circle represents one mouse) represent the % entries in the open arms over the total number of entries, and the % time spent in open arms. cKO mice enter open arms more frequently than WT animals ($*p < 0.05$, Student's t-test), while the amount of time spent in the open arms is comparable among the two genotypes. **C.** Results for Kidins220$^{+/+}$ (n = 13, cyan) and Kidins220$^{lox/lox}$ (n = 11, orange) mice. The % entries in the open arms and the % time spent in open arms are comparable between the two genotypes ($p > 0.05$, Student's t-test). Data are represented as mean  s.e.m. in all panels.

### II.I.3 Open field

The 'open field' test is based on the same principle as the EPM, i.e. that open spaces elicit anxiety on mice. The level of anxiety is extrapolated from the amount of time the mice spend in the centre of the open field, whereby a high level of anxiety will be reflected in more time spent outside the centre and closer to the external walls **Figure 11 3A.** As shown in **Figure 11 B** (data from Dr Sathapathy), cKO mice consistently spent more time in the central zone of the open field. In contrast, Kidins220$^{lox/lox}$ mice did not show this trend in behaviour (**Figure 11 C**). The behaviour of WT and Kidins220$^{+/+}$ mice is significantly different and discussed in section III.III.

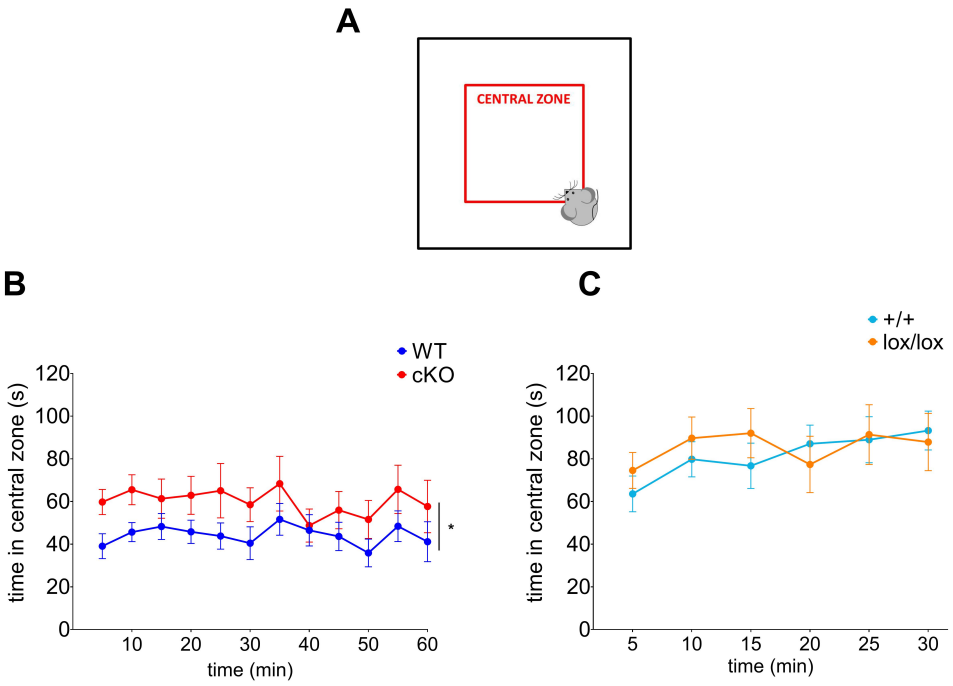


Figure 11. **Open field A.** Schematic representation of the open field; the central zone is highlighted in red. **B.**Results for WT (n = 21, blue) and cKO (n = 21, red) mice. The amount of time the mice spent in the central zone during the test is plotted, divided into 5 min bins. cKO mice spent consistently more time ($F_{1,37} = 4.568; *p < 0.05$ genotype effect, RM-ANOVA) than WT in the central zone. **C.** Results for Kidins220$^{+/+}$ (n = 14, cyan) and Kidins220$^{lox/lox}$ (n = 11, orange) mice. In this case, the behaviour is comparable among the two genotypes. ($F_{1,21} = 0.1164; p > 0.05$ genotype effect, RM-ANOVA). Data are represented as mean s.e.m. in all panels.

### II.I.4 Social habituation/dis-habituation

In this test, social interaction and social discrimination are tested (**Figure12 A**). This test is based on the increment of interest that social novelty entails in mice. Therefore, social recognition is extrapolated from the amount of time the test mouse explores the stimulus mouse. The social interaction behaviour is assessed during the first 4 trials, where the tested mouse interacts freely with the same mouse (familiar mouse). The social discrimination capability is tested in trial 5 when the stimulus mouse is a different one. An increment in the social interaction during trial 5 will indicate that the tested mouse differentiates the novel mouse from the familiar one. To evaluate social memory, the time the test mouse spent sniffing the familiar and the novel mice was evaluated across all trials. As shown in (**Figure 12 B**), cKO mice interacted significantly more with the familiar mouse compared to WT animals over the first four trials (**left and middle** panels), however, their interest for the novel mouse during the $5^{th}$ trial was significantly reduced compared to WT (**right** panel). When tested with the same protocol, instead, the behaviour of Kidins220$^{lox/lox}$ mice was comparable to the one of Kidins220$^{+/+}$ animals across all the trials (**Figure 12 C**).

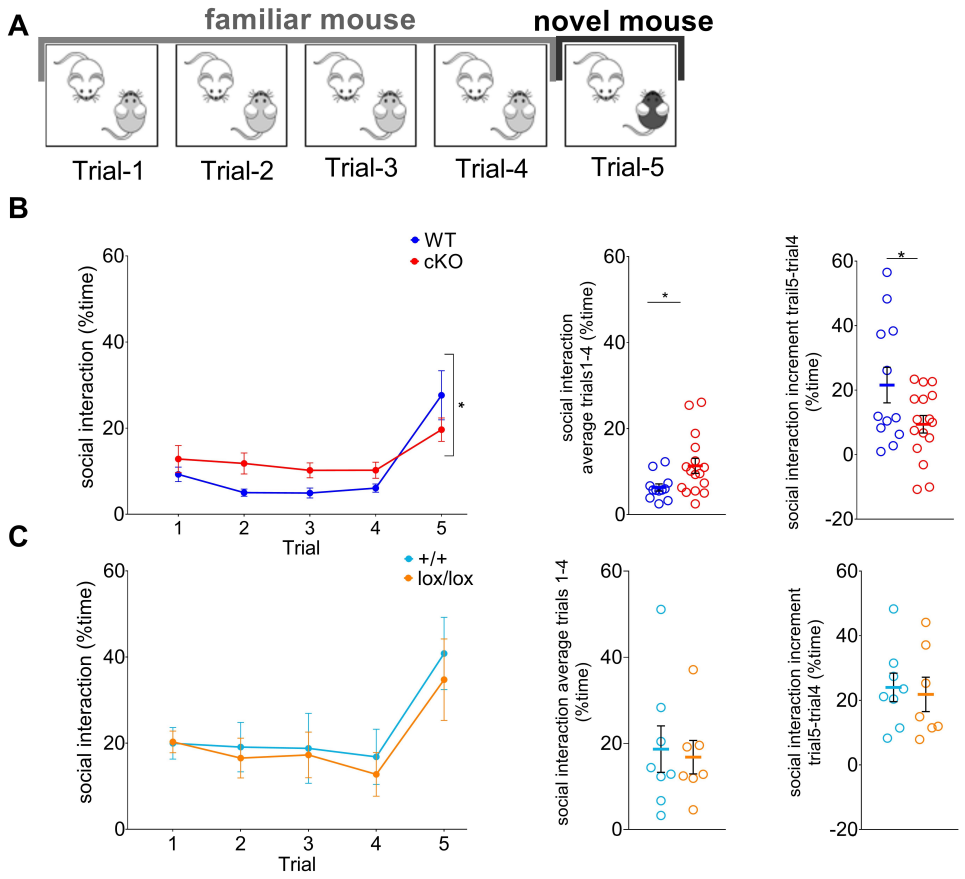


Figure 12. **Social habituation A.** Schematic representation of the test protocol, which consisted of 5 trials of 1 min, separated by inter-trial-intervals (ITI) of 3 min.**B.** Results for WT (n = 12, blue) and cKO (n = 16, red) mice. **Left**: the % time mice were engaged in social interaction in each trial is reported. Animals from both genotypes showed a significant increase in the social interaction in the 5th trial (trial effect: $F_{4,104} = 18.17, ****p < 0.0001$ RM-ANOVA, not indicated in the graph). A significant interaction (indicated in the graph) between genotype and trials indicates different behaviour between cKO and WT (Interaction: $F_{4,104} = 3.458, *p < 0.05$ RM-ANOVA. **Middle**: the average social interaction throughout the first 4 trials is reported. Each circle corresponds to an individual. cKO mice spent significantly more time than WT animals interacting with the familiar mouse. ($*p < 0.05$, Students t-test). **Right**: The difference in social interaction between the 5th and the 4$^{th}$ trial is represented. cKO mice display less interest for the novel mouse compared to WT animals ($*p < 0.05$, Students t-test).**C.** Results for Kidins220$^{+/+}$ (n = 8, cyan) and Kidins220$^{lox/lox}$ (n = 7, orange) mice. **Left**: Animals from both genotypes showed a significant increase in the social interaction in the 5$^{th}$ trial, indicated in the graph (trial effect: $F_{4,52} = 11.74, ****p < 0.0001$ RM-ANOVA). **Middle and left**: the amount of social interaction of Kidins220$^{lox/lox}$ mice is comparable to the one of Kidins220$^{+/+}$ animals across all trials. ($p > 0.05$, Students t-test). Data are represented as mean  s.e.m in all panels.

### II.I.5 Social memory

To better define the social memory deficits shown by cKO mice, we performed an additional test to assess long-term social memory, which consisted in two 5 min trials of free social interaction separated by a 1 h inter-trial-interval (ITI) (**Figure 13 A**). Surprisingly, the performance of WT and cKO mice in this test was comparable (**Figure 13 B**), in contrast to the results of the social habituation test, previously described. Of note, we could not use Kidins220$^{+/+}$ male animals in this test, as they showed a high level of aggressiveness when put in the same cage with a novel mouse. Thus, Kidins220$^{lox/lox}$ animals were compared to WT. When the stimulus mouse of the 2$^{nd}$ trial is the same as the one used in the 1$^{st}$ trial (**Figure 13 B, top**), a decrease in social interaction in the second trial is expected, as the tested mouse is expected to remember the other animal (i.e. long-term social memory) and consequently have less social interest. WT mice show a tendency towards decreasing the social interaction, unlike their cKO littermates. The Kidins220$^{lox/lox}$ mice show the opposite trend and a bigger inter-subject variability. When the stimulus mouse of the 2$^{nd}$ trial is different from the one used in the 1$^{st}$ trial (**Figure 13 B, bottom**) the social interaction is instead expected to be constant.

We also analysed the mating behaviour of our mutant mice (**Figure 13 C**). The tested mice were always the males (either WT or cKO). The stimulus females were WT and in the reproductive stage of the oestrous cycle. In this case, since Kidins220$^{lox/lox}$ animals did not show any social deficits in the previous tests, we performed this analysis only on cKO mice. We measured the time male cKO and WT animals spent sniffing a novel WT female that is introduced in their cage for the first time and during 5 min. As shown in **Figure 13 D**, the mating behaviour was comparable between WT and cKO animals.

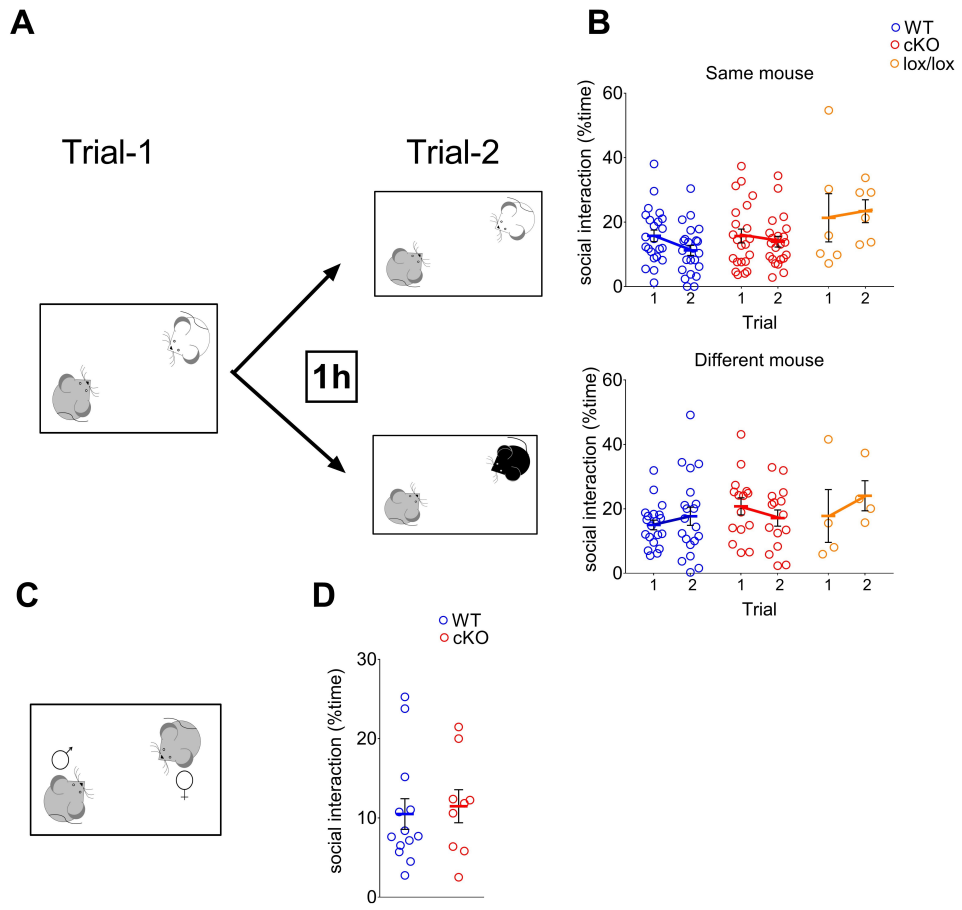


Figure 13. **Social memory A.** Schematic representation of the test. The mice are left in the same cage for 5 min, and the ITI Is of 1 h. The second trial is performed with the same stimulus mouse or a different one.**B.** Results for WT (n = 23, blue), cKO (n = 22, red) and Kidins220$^{lox/lox}$ (n=6, orange) mice. Each circle represents an individual.**Top:** the % time sniffing the stimulus mouse when it is the same in both trials is shown. The % time spent sniffing the stimulus mouse is reported for each trial and for each genotype (no statistically significant effects detected $p < 0.05$, RM-ANOVA).**Bottom:** the % time sniffing the stimulus mouse when it is different between trials is shown (no statistically significant effects detected, $p < 0.05$ RM-ANOVA).**C.**Schematic representation of the male-female interaction test. The test lasted 5 min.**D.** Results for WT (n =13, blue) and cKO (n = 9, red) mice. The % time WT and cKO males spent sniffing a novel WT female is reported. No difference was found between the two genotypes ($p > 0.05$, Student's t-test). Data are represented as mean  s.e.m in all panels.

### II.I.6 Olfactory ability

An important component of social behaviour is the ability of animals to discriminate odours, in particular, social versus non-social odours. To address this point, we performed the olfactory ability test on cKO (**Figure 14 A**) and Kidins220$^{lox/lox}$ (**14 B**) mice. The odours were presented to the mice in cotton swabs dipped in the different smells. The time spent by each animal sniffing the cotton swab was evaluated across all trials. This test allows assessing 3 different parameters: odour differenciation, olfactory habituation to smells and social odour discrimination. The expected behaviour of a healthy control mouse (see the behaviour of mice from all genotypes in **Figure 14**) is an increase in the time sniffing an odour the first time it is presented (trial 1) and a subsequential decrease on the sniffing time during the following exposure to the same smell (trials 2 $\&$ 3). These parameters are determined by the interest the mouse feels for a novel odour, which is translated to an increment in the amount of time spent sniffing the cotton swab, while during the subsequent trials the mouse experiences a reduced interest for odours that are already known. Odour differentiation and olfactory habituation indicate the correct functioning of the olfactory system. The social odour discrimination is observed in the significant increment of time sniffing smells coming from other mice (see the behaviour of the WT and Kidins220$^{+/+}$ mice in **Figure 14**), compared to the time spent sniffing neutral smells (water, strawberry and cinnamon). All the genotypes showed olfactory habituation and intact olfactory memory to non-neutral smells, thus indicating that the olfactory system of all mice is not impaired. However, when social odours are presented, WT and Kidins220$^{+/+}$ mice showed highly increased sniffing time, as expected for this type of smell, while interestingly, cKO and Kidins220$^{lox/lox}$ mice spent the same amount of time investigating the social odours and the neutral ones.

### II.I.7 Pre-pulse inhibition and startle response

Sensory-motor gating deficits are correlated to disorders like ASD and schizophrenia. These deficits are tested by assessing the inhibition of the acoustic startle when preceded by a weak stimulus (pre-pulse inhibition, see **Figure 15 A**), and by as-

sessing the startle response to acoustic stimuli of different intensities (**Figure 15 B**). The inhibition of the startle response elicited by pre-pulses is comparable between WT and cKO animals across all the tested intensities (**Figure 15 A, left**). However, we noticed that in the absence of pre-pulse, cKO mice displayed a trend towards a reduction of the acoustic startle in response to the most intense stimulus (120 dB). This genotype effect in sensorimotor response to startle was confirmed by performing the startle response test, which showed that the startle response to 110 and 120 dB stimuli is significantly lower in cKO mice (**Figure 15 B**). The same experiments are presently ongoing for Kidins220$^{+/+}$ and Kidins220$^{lox/lox}$ mice.

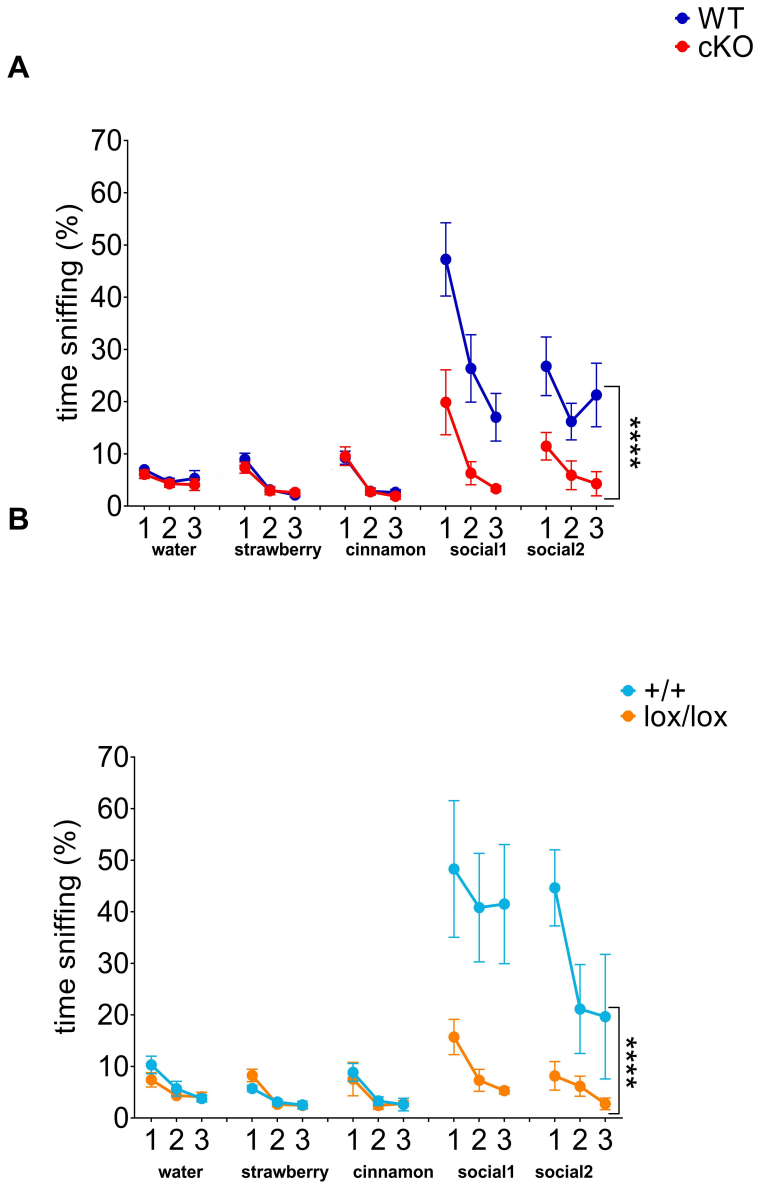


Figure 14. **Olfactory ability** The olfactory ability results are expressed as the % time each mouse spent sniffing the cotton-swab in the presence of different smells, as indicated.**A.** Results for WT (n = 19, blue) and cKO (n = 12, red) mice. Mice from both genotypes habituated equally to each smell and distinguished each new smell from the previous (trial effect:$F_{14,448} = 14.25 * * * * p < 0.0001$ RM-ANOVA Asterisks are not indicated for clarity). WT mice showed a significantly higher interest for social odours, unlike cKO mice, so the interaction between the genotype and the smell is significant ($F_{14,448} = 4.354 * * * * p < 0.0001$ genotype effect, RM-ANOVA Sidak's multiple comparisons post-hoc test between WT and cKO indicated statistically significant differences at all trials within the 'social1' and 'social2' odours. Asterisks are not indicated for clarity). **B.** Results for Kidins220$^{+/+}$ (n = 6, cyan) and Kidins220$^{lox/lox}$ (n = 7, orange) mice. Mice from both genotypes habituated equally to each smell and distinguished each new smell from the previous (trial effect: $F_{14,154} = 9.201 * * * * p < 0.0001$ RM-ANOVA followed by Sidak's multiple comparisons post hoc test. Asterisks are not indicated for clarity). Kidins220$^{+/+}$ mice showed significantly more interest for the social smells opposed to Kidins220$^{lox/lox}$ littermates, so the interaction between the genotype and the smell is significant (interaction: $F_{14,154} = 5.494 * * * * p < 0.0001$ RM-ANOVA followed by Sidak's multiple comparisons test $* * * * p < 0.0001$ for social1 trial-1 for social2. Asterisks are not indicated for clarity). Data are represented as mean  s.e.m. in all panels.

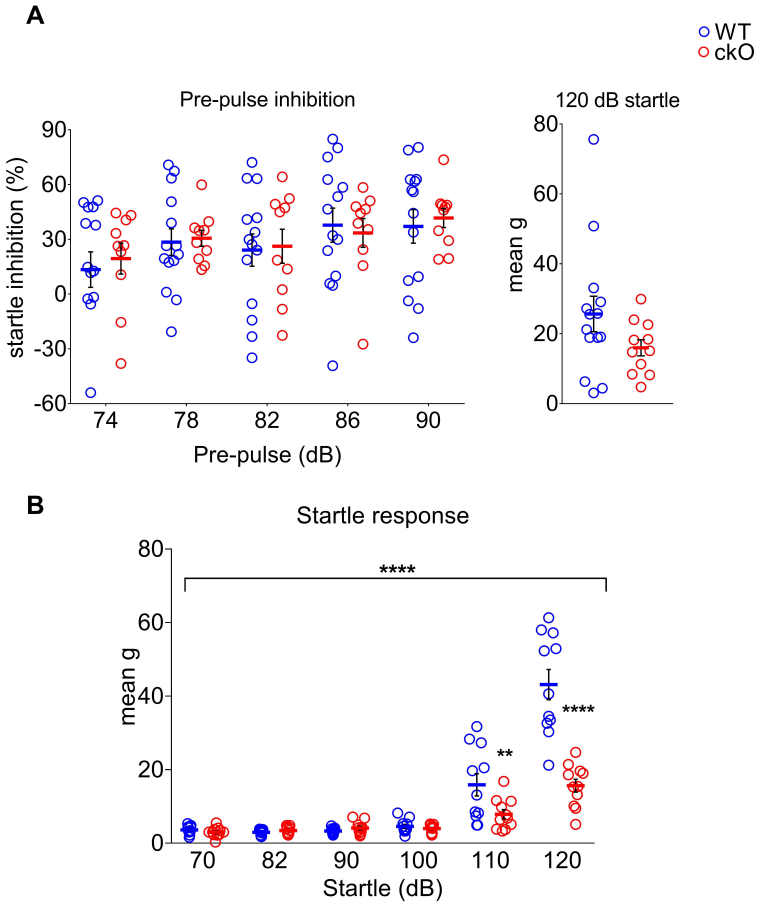


Figure 15. **A. Pre-pulse inhibition.** Results for WT (n = 14, blue) and cKO (n = 11, red) mice. The % inhibition of the startle response induced by pre-pulses of different intensities (74, 78, 82, 85 or 90 dB) is calculated by using the formula: Startle response inhibition=$[100 - \frac{mean of the PPI_{74 or 78 or 82 or 86 or 90}}{startle response}]x100$, and it is comparable between the two genotypes. WT and cKO mice show the expected increment of startle response inhibition with increasing pre-pulse intensity ($F_{4,88} = 6.26, ***p < 0.001$, RM-ANOVA). Circles represent the values of single individuals. **B. Startle response.** Results for WT (n = 14, blue) and cKO (n = 13, red) mice. The startle response to each auditory stimulus (70, 82, 90, 100, 110 or 120 dB) is evaluated as mean g. The increasing intensity of the startle affected the motor startle response of both genotypes (trial effect: $F_{5,100} = 87.3 ****p < 0.0001$ RM-ANOVA, asterisks not indicated). Values are significantly lower in cKO mice compared to their WT littermates for high intensity stimuli, so there is a significant genotype-trial interaction. (interaction: $F_{5,100} = 24.79, **** p < 0.0001$, RM-ANOVA followed by Sidaks multiple comparisons post-hoc test $**p < 0.01 ****p < 0.0001$ at 1000 and 120 dB, respectively). Data are represented as mean  s.e.m. in all panels.

## II.II Role of Kidins220 in adult brain morphology

Previous data by Dr Satapathy had addressed the question of whether, besides its well-known role in modulating neuronal survival and differentiation during embryogenesis, Kidins220 plays a role in the maintenance of neuronal morphology also in the adult brain. In this work, I completed this analysis and extended it to include the Kidins220$^{lox/lox}$ mice.

### II.II.1 Brain morphology

Kidins220$^{-/-}$ embryos display a marked enlargement of brain ventricles [31]. Here, we measured brain ventricles in both cKO and Kidins220$^{lox/lox}$ animals, at 2-3 month of age (**Figure 16 A**). The volume of the lateral and third ventricles was estimated from serial brain sections obtained from cKO and WT, Kidins220$^{+/+}$ and Kidins220$^{lox/lox}$ littermates. As can be appreciated in the representative images (**right**) and in the corresponding quantification (**left**) cKO mice are characterized by a marked enlargement of ventricles. A similar trend was observed in the brain of Kidins220$^{lox/lox}$ animals, which however was not statistically different from Kidins220$^{+/+}$ mice.

### II.II.2 Neuronal morphology

Dendritic branching of cKO mice was previously measured in the motor and sensory cortex of cKO brains, finding a reduced dendritic arborisation in the motor cortex of cKO mice (see introduction). Here, this analysis was extended to granule cells of the dentate gyrus (DG) of the hippocampus of WT and cKO littermates. Golgi-stained brains were sectioned and single neurons analysed by Sholl analysis. A significant interaction between the genotype and the number of intersections at each radius was detected in the DG neurons, indicating more complex and longer denrites in DG neurons of the cKO mice (**Figure 16 B**).

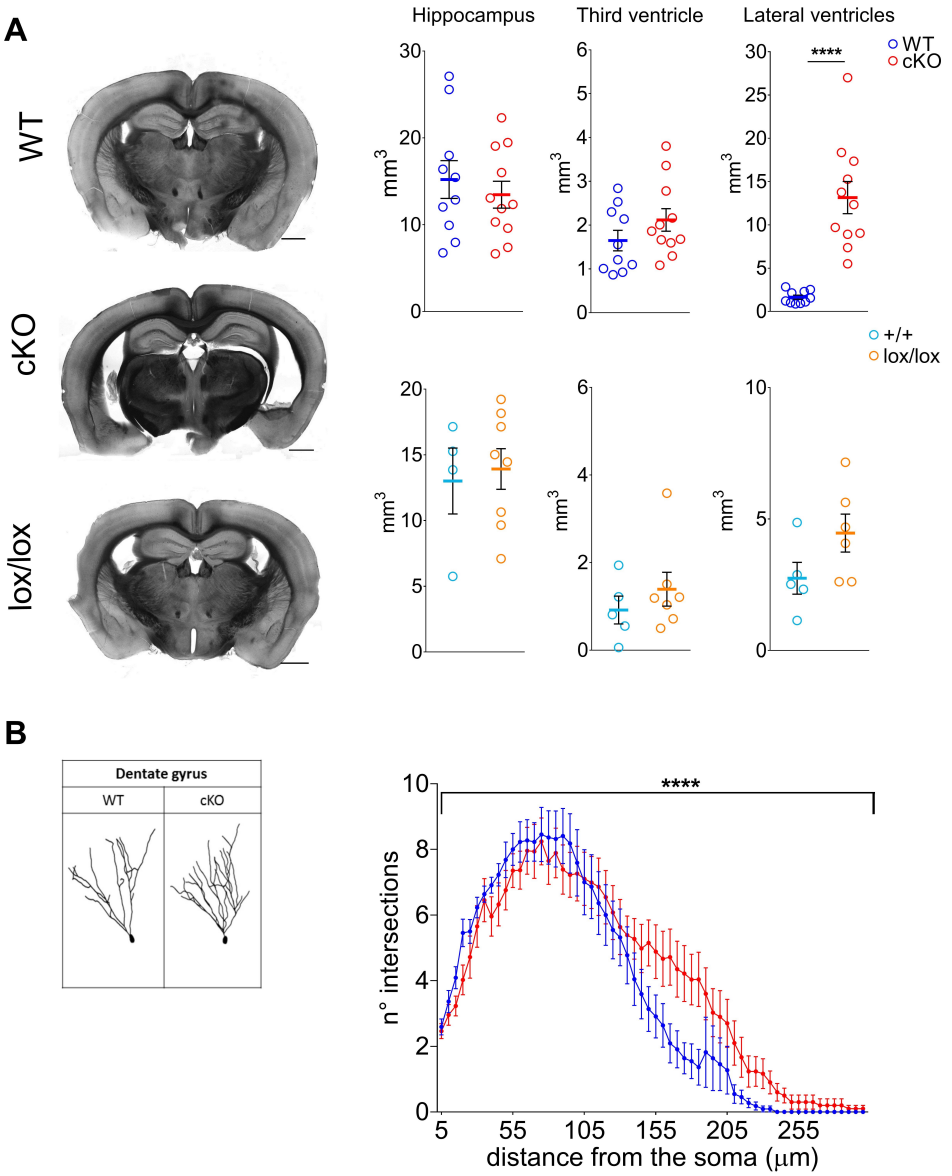


Figure 16. **Brain histological analysis A. Left** representative brain slices from WT, cKO and Kidins220$^{lox/lox}$ mice (scale bars, 1 mm); Kidins220$^{+/+}$ samples were identical to WT (not shown). **Right:** hippocampus, third and lateral ventricles volumes are shown. The volume of the lateral ventricles of cKO mice is significantly larger than that of WT. WT: n= 10; cKO: n= 11; Kidins220$^{+/+}$ : n= 5; Kidins220$^{lox/lox}$ : n= 8 ($****p < 0.0001$, Student's t-test).**B. Left:** representative neurons from WT and cKO dentate gyrus, and **Right:** Sholl analysis data. A significant interaction between genotype and trial effect was found ($F_{59,1121} = 2.21$ RM-ANOVA $****p < 0.0001$, indicated in the graph). 3-10 neurons per animal were analysed, from WT n= 11, cKO n=10 animals. Data are represented as mean  s.e.m. in all panels.

## II.III Putative influence of Cre expression on behaviour

The Cre recombinase/lox system is commonly used for the generation of total and conditional knockout and knock-in mouse models. Animals bearing the Cre transgene are commonly regarded as wild type, however they express an exogenous protein for a prolonged amount of time in their embryonic and/or adult life, depending on the promoter used, and the possibility of Cre being a factor of variability *per se* should therefore not be disregarded. In the mouse model used in this project, the Cre enzyme is expressed under the promoter of CaMKII, which is active in forebrain excitatory neurons from P14 and throughout the rest of the animal's life (see **Figure 6**, Introduction). To address this issue, here the behavioural results from the two groups used as controls (Kidins220$^{+/+}$ and WT) are presented. As shown in the crossing plan (see materials and methods), the WT littermates of the cKO mice are Kidins220$^{+/+}$ ; +/cre, which is the proper control group as cKO animals are Kidins220$^{lox/lox}$ ; +/Cre. Nevertheless, when the results from WT vs cKO and those from Kidins220$^{+/+}$ vs Kidins220$^{lox/lox}$ were put together, substantial differences in the behaviour of WT and Kidins220$^{+/+}$ animals were evident in some tests.

In the fear conditioning test, a genotype effect was seen during the '*novel context + cue* ' trial, where the cued fear is tested. Interestingly, WT (+/Cre) displayed increased freezing compared to Kidins220$^{+/+}$ across the baseline, cue, and post-cue phases (see **Figure 17 A, right**).

In the open field test, Kidins220$^{+/+}$ mice spent consistently more time than WT in the central zone (**Figure 17 B**), while the performance of the two genotypes was comparable in the EPM test, in terms of both n. of entries and time spent in the open arms (**Figure 17 C**).

Differences between Kidins220$^{+/+}$ and WT(+/Cre) were also found in the social habituation / dis-habituation test. Here, Kidins220$^{+/+}$ showed consistently more social interaction in all the trials of the test, however, the social memory was preserved, as mice of both genotypes displayed increased interest for the novel mouse (**Figure 17 A**). The olfactory memory results were also compared and no significant differences were seen among the two genotypes (**Figure 18 B**).

Even though significant differences are found in the behaviour of WT(+/Cre) compared to Kidins220$^{+/+}$ , a causal role of Cre in the observed effects is still not certain. Indeed, a potential effect of altered maternal care should not be discarded. WT(+/Cre) mice are usually gestated by female mice (+/lox; Cre/Cre) and born into litters with Het and cKO siblings. The impact that these breeding characteristics may have on the single animal must be taken into account when comparing WT(+/Cre) mice with Kidins220$^{+/+}$ mice, which are gestated by Kidins220$^{+/lox}$ mothers and born into litters of Kidins220$^{+/lox}$ and Kidins220$^{lox/lox}$ mice.Indeed, the effect of maternal care in behaviour was observed in [71] among other investigation projects. Thus, we hypothesize that the observed behavioural variability could be ascribed to specific cellular effects triggered by prolongued Cre expression, and/or to alterations in paternal care and in the interaction with siblings of different genotypes, which the Cre-expressing animals experience throughout their life.

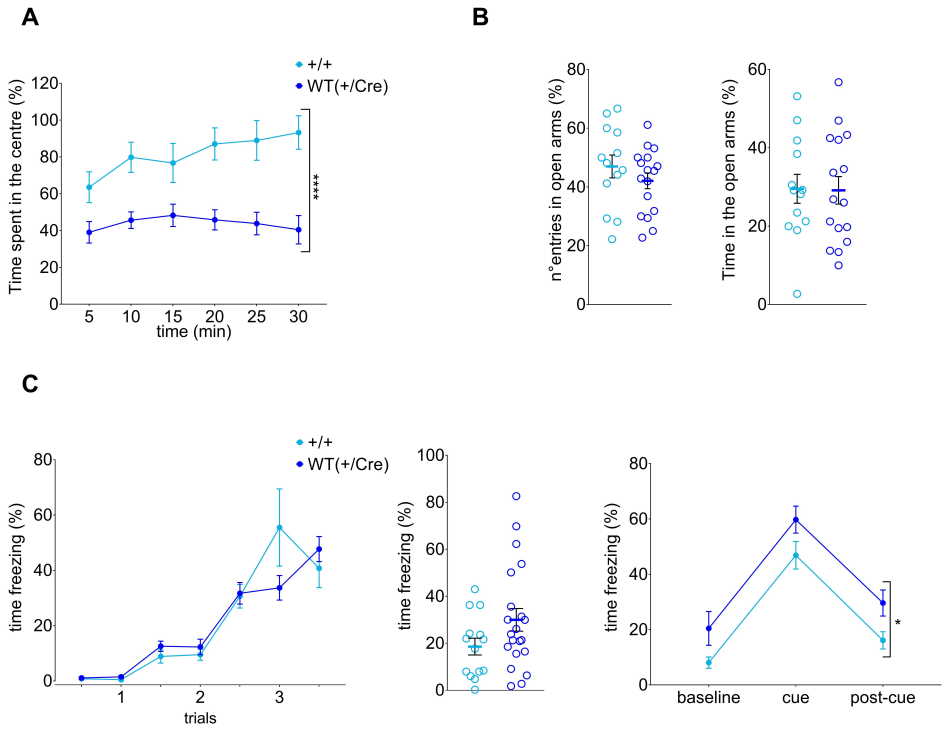


Figure 17. **A. Open field.** Results from Kidins220$^{+/+}$ (n = 12, cyan) and WT(+/Cre)(n = 21, blue) are shown. The amount of time the mice spent in the central zone during the test is plotted, divided into 5 min bins. Kidins220$^{+/+}$ mice spent consistently more time in the central zone than the WT (+/Cre) (genotype effect: $F1, 31 = 24.32 * * * * p < 0.0001$, RM-ANOVA). **B.Elevated plus maze.** Results from Kidins220$^{+/+}$ (n = 13 cyan) and WT(+/Cre)(n = 17 blue) are shown. The % entries in the open arms and the % time spent in open arms are comparable between the two genotypes ($p > 0.05$, Student's t-test). **C. Fear conditioning.** Results from Kidins220$^{+/+}$ (n = 14, cyan) and WT(+/Cre)( n = 21, blue) are shown. The amount of time the mice spent freezing during each phase of the experiment is shown as % freezing time. In the *novel context + cue* phase, WT(+/Cre) froze more than Kidins220$^{+/+}$ (genotype effect:$F_{1,31} = 5.619 * p < 0.05$, RM-ANOVA). Results are represented as mean s.e.m in all panels.

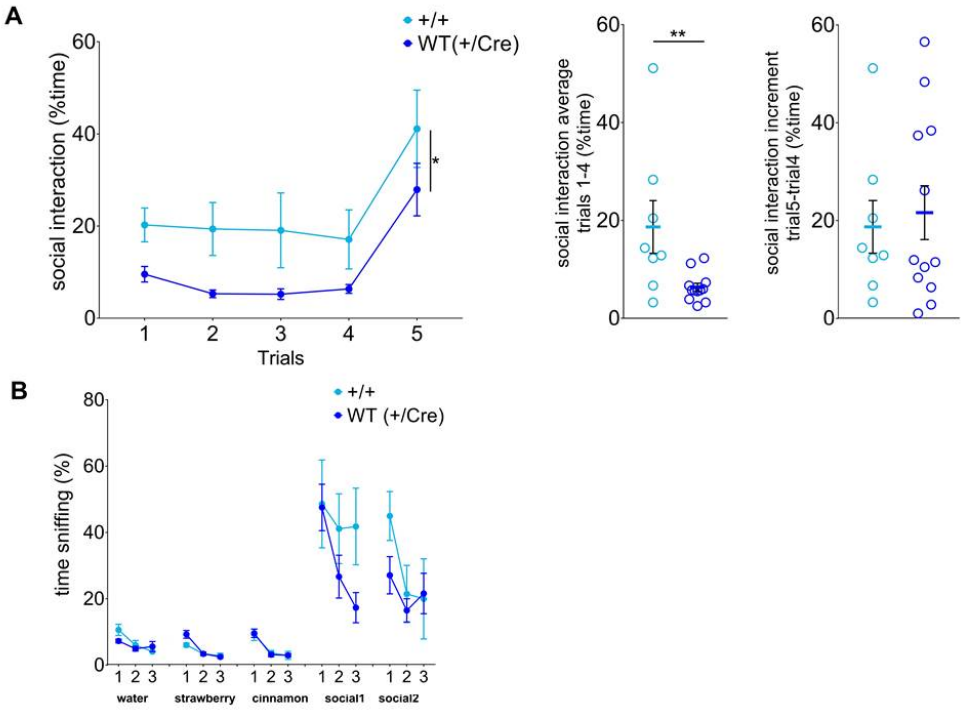


Figure 18. **A.Social habituation/ dis-habituation.** Results for Kidins220$^{+/+}$ (n = 8, cyan) and WT(+/Cre)(n = 12, blue) mice. **Left:** The % time mice were engaged in social interaction in each trial is reported. Kidins220$^{+/+}$ mice interacted more than the WT(+/Cre) mice ($F_{1,18} = 6.53 * p < 0.05$ genotype effect, RM-ANOVA). **Middle:** the average social interaction throughout the first 4 trials is reported. Each circle corresponds to an individual. Kidins220$^{+/+}$ mice spent significantly more time than WT animals interacting with the familiar mouse ($** p < 0.01$, Mann-Whitney test). **Right:** The difference in social interaction between the 5th and the 4th trial is represented. The increment of social interaction between trial 5 and trial 4 is comparable among genotypes ($p > 0.05$, Mann-Whitney U test). **B.Olfactory ability.** Results for Kidins220$^{+/+}$ (n = 6, cyan) and WT(+/Cre)(n = 22, blue). The olfactory habituation results are expressed as the % time each mouse spent sniffing the cotton-swab. The behaviour of cyan the two genotypes is comparable ($F_{1,25} = 1.27, p > 0.05$, RM-ANOVA). Results are expressed ad means.e.m. in all panels.

# III Discussion

## III.I behavioural tests

A panel of behavioural tests has been performed with the Kidins220 cKO and Kidins220$^{lox/lox}$ mice. The behavioural characterization was guided by the growing body of literature identifying Kidins220 as a risk factor for complex psychiatric disorders like ASD and schizophrenia. The behavioural tests were performed also on the Kidins220$^{lox/lox}$ animals in order to discern which behavioural phenotypes were due to the absence of Kidins220 in the excitatory neurons of the forebrain, and which ones were due to the exclusive expression of the Kidins220 full-length isoform (m1), which is characterizing the Kidins220$^{lox/lox}$ mice. The clear impairment in social olfactory recognition is the only phenotype shared by the two genotypes. Kidins220 cKO mice are characterized by a social discrimination deficiency and reduced startle response to auditory stimuli. In addition, they show reduced anxiety in the 'open field' and 'the elevated plus maze test'. cKO females have impaired spatial memory, as shown by the results of the Morris water maze and fear conditioning tests. Kidins220$^{lox/lox}$ mice show comparable performance to the Kidins220$^{+/+}$ mice in all these tests (the Morris water maze test was not performed with these mice because of technical issues, and the startle response test is in progress).

### III.I.1 Social olfaction and social discrimination impairment and reduced startle response

The 'olfactory ability' test shows a clear impairment in social odour discrimination in both cKO and Kidins220$^{lox/lox}$ mice. The expected habituation to each smell across the trials and the discrimination between each smell, indicate the correct functioning of the olfactory system in these mice. Therefore the olfactory impairment affects specifically the recognition of odours from co-specific animals. This is indicative of the relevance of Kidins220 isoforms for the correct codification of social odours in adult mice. As previously explained (see **Introduction**), the difference between cKO and Kidins220$^{lox/lox}$ mice is the absence of Kidins220 in the excitatory neurons of the

forebrain of the cKO mice. What they have in common is the exclusive expression of a full-length isoform of Kidins220 (m1, FL) everywhere else. The recently described SINO syndrome in humans proves the value of the correct expression of Kidins220 splicing isoforms, and the severe consequences that their absence entails [63, 65]. It is probable that the different protein-interaction domains present in each Kidins220 isoform is the reason for their specific location and differential expression during development. Moreover, neurotrophins appear to have a key role on the timing of this expression [38].

Among the multiple and diverse signalling pathways Kidins220 is involved in, it was found to interact with sodium channels. Sodium channels are fundamental players in neuronal communications. They are multimeric complexes of $\alpha$ and $\beta$ subunits that exist in several isoforms and their functional characteristics depend on which subunits compose each channel. Sodium channels as $Na_v$ 1.2 and $Na_v$ 1.9 are known to be modulated by BDNF [36]. In fact, Kidins220$^{-/-}$ hippocampal GABAergic neurons display a higher $Na^+$ conductance [36]. In addition, MEA (Multi Electrode Arrays) recordings of mouse hippocampal cultures indicated impairment in the polysynaptic and reverberant propagation of excitation in neuronal networks lacking Kidins220 [36]. During this same work, the direct interaction between Kidins220 and the sodium channel $Na_v1.2$ was observed. $Na_v1.2$ channels are subject to dynamic regulation by tyrosine phosphorylation/dephosphorylation events upon TrkB activation, which leads to increase their fast inactivation by Fyn kinase [72]. This points towards the role of Kidins220 as an intermediary between Trk neurotrophin receptors and the downstream modulation of sodium channels activity [36]. Therefore, Kidins220 is probably located upstream from $Na^+$ in this signalling pathway.

Olfaction is a major modality through which animals may detect and identify conspecifics. The olfactory system is key for mice survival and social behaviour. For example, scent marking and counter-marking of the scent marks of other males are important components of dominance advertisement among male house mice, and strongly influence their aggressive interactions. In addition, females respond to male urinary pheromones in a variety of ways that enhance their reproductive success, including early induction of puberty and the capacity of activating the same neuroen-

docrine mechanisms resulting in loss of pregnancy [73]. The detection of odourants is registered by two distinct chemosensory systems originating in the nose: the main olfactory system (MOS) with receptors that encode signals to the main olfactory bulbs (MOB), and the vomeronasal organ (VNO) composed of axons connecting with the accessory olfactory bulb (AOB), an anatomically independent region in the posterior part of the olfactory bulb. The AOB and MOB give rise to separate pathways that terminate in both separate and overlapping areas of the basal telencephalon. From the amygdala, vomeronasal pathways project to the medial preoptic area and the ventromedial nucleus of the hypothalamus. Selective disruption of the MOB, leaving the accessory system functionally intact, has only a minor effect on aggression, but completely disrupts mating behaviour in male mice. Removal of the VNO alone does not affect mating behaviour, but markedly reduces scent marking responses and aggressive behaviour to other male mice [74]. $Na_v$ channel isoforms are distributed in specific locations of the olfactory system, being $Na_v1.7$ the most abundant subtype not only in the MOS but also in the VNO, and $Na_v1.2$ and $Na_v1.6$ specifically located in sensory neuron subpopulations of the VNO [75].

The Kidins220 cKO mice show no impairment in mating behaviour but fail to distinguish between social and non-social odours, as the Kidins220$^{lox/lox}$ mice do. Interestingly, this phenotype is in line with the effects caused by VNO ablation in mice. $Na_v1.2$ channels are expressed in the soma of the vomeronasal sensory neurons of the VNO basal layer [75]. Therefore it is possible that the absence of m6, one of the two brain-specific Kidins220 isoforms [38], leads to an inhibitory/excitatory unbalance due to the impaired regulation of sodium channels upon neurotrophic signalling, eliciting a defective encoding of social odours by the VNO. The preliminary results of the DHF treatment on the 'olfactory ability test', where social odour discrimination seems to be rescued by the treatment, point towards the involvement of BDNF. It has been reported that BDNF and TrkB deficiencies non-specifically affect the discrimination of all odours [76]. Therefore, the aforementioned role of Kidins220 as a modulator of sodium channels appears to be of great relevance for social odours discrimination, and interestingly, this seems to by linked to BDNF signalling. The rescue experiment results also reveal an interesting trend of differential effects of

7,8-Dihydroxyflavone (DHF) on males and females (see **Figure 19 A, B** in **Future perspectives** section IV.I). Social odour discrimination in females seems to be more effectively rescued than in males. Indeed it has been previously reported that female olfactory system is generally more effective than the male one, and the molecular basis of these sensory differences could be partly related to differences in the endocrine status [77]. odourant presentation in females elicits olfactory sensory neurons (OSN) input into a broader range of olfactory bulb glomeruli and this input occurs earlier in the odour presentation compared to males [77]. Moreover, sex hormones modulate BDNF signalling in different ways in males and females. The BDNF gene contains an estrogen-response element, which establishes a positive correlation between estrogen and BDNF expression [78]. Conversely, testosterone has a decreasing effect on BDNF-TrkB signalling during adolescence [79]. Given these sex-specific characteristics, the action of DHF is probably more effective in the females VNO, which would favour plasticity upon BDNF-signalling increment. In addition, given that the lack of Kidins220 isoforms is likely to impair BDNF signalling, the effect of testosterone on this neurotrophin and the TrkB receptor during adolescence might entail VNO circuit defects not modifiable by DHF treatment. Social recognition is impaired in Kidins220 cKO mice, in line with the social odour discrimination impairment shown by this genotype. The fact that Kidins220$^{lox/lox}$ mice do not show the same impairment indicates that this phenotype is caused by the absence of Kidins220, rather than by an unbalance in its isoform expression. Moreover there were no significant differences between Kidins220$^{lox/lox}$ males and females in neither of the two tests. Kidins220$^{lox/lox}$ mice showed comparable social recognition to their Kidins220$^{+/+}$ littermates, underlying the relevance of the expression of Kidins220 in the forebrain for social behaviour. Therefore differences in 'olfactory ability test' and 'social habituation test' indicate involvement of different, yet some overlapping, brain circuits. In the work published by Ferguson and colleagues [80], mice lacking the oxytocin gene showed social recognition impairment when tested in the same social habituation paradigm as the one used during this project, as the vasopressin receptor V1a KO mice did [81]. A key role of oxytocin receptors in the aDG-CA2/CA3 hippocampal axis was later identified by Raam and coleagues [82]. Additionally, BDNF and its

receptors are highly expressed in the paraventricular nucleus (PVN), were neurons synthetizing oxytocin are located. In fact a disruption of BDNF signalling may lead to increased inhibition onto oxytocinergic neurons that could alter the timing or levels of oxytocin release, with an appreciable impact on social behaviours [78]. Moreover, the reduced startle response shown by cKO mice is also in line with the putative interaction between oxytocin, BDNF and Kidins220; indeed, oxytocin KO mice have reduced startle response [80].

The involvement of the hippocampal DG in the social recognition circuitry provides the connection between the differential dendrite ramification found by Sholl analysis in the brain area and the social recognition impairment of Kidins220 cKO mice. Oxytocin has been largely proposed as an important element for the understanding of complex disorders as ASD and schizophrenia [83]. In parallel, the decreased BDNF expression induced by testosterone in adolescent males has been proposed as a risk factor for the development of chronic schizophrenia [79]. The marked social impairments in ASD and schizophrenia and the crucial role of oxytocin in social cognition indicate that oxytocin is a promising treatment target for these disorders. Kidins220 interaction with BDNF, which in turn is a regulator of oxytocin signalling [78], makes Kidins220 one genetic risk factor to take into account in order to diagnose and treat these complex disorders.

### III.I.2 Contextual memory impairment in cKO females

The results obtained in the Morris water maze and in context trial of the fear conditioning test reveal impaired spatial memory in Kidins220 cKO females. Our data are in line with the published literature, as spatial memory deficits were also identified in ARMS$^{+/-}$ females, which showed a reduced performance in the training trial of the Morris water maze [69]. This sex-specific impairment may point towards estrogen functions in learning and memory. During the last decades, the involvement of 17-estradiol ($E_2$) in the regulation of learning and memory in male and female rodents has been established. Ovariectomy itself impairs some forms of memory including spatial reference memory in the water maze, and systemic $E_2$ given acutely

or chronically improves spatial working memory. Interestingly, the primary endogenous source of E2 for hippocampal neurons in both males and females is probably the neuronal and glial hippocampal population itself. Indeed, systemic injection of $E_2$ synthesis inhibitor letrozol is associated with impaired long-term potentiation (LTP) and transient dephosphorization of cofilin in male and female rats, although these deficits are more striking in females. Not only LTP becomes deficient, but also spine density and variety decreases more in females than in males. In addition, $E_2$ acts on learning and memory by activating the ERK signalling pathway [84]. It will be interesting to address the question of whether such deficiency is exclusively linked to BDNF signalling, or whether estrogen signalling is also impaired, and if so, whether this is more relevant in females.

#### III.I.3 Reduced-anxiety behaviour

Kidins220 cKO mice show reduced anxiety-like behaviour in the open field and the elevated plus maze tests in the absence of hyper locomotion. This behavioural characteristic has been described in diverse mouse models as the CamKII-driven Cre BDNF cKO [85], the CamKIV KO [86], and the vasopressin V1a (V1aR) receptor KO mice [81]. On the other hand, mouse models expressing the BDNF Val66Met allele in homozygosity display enhanced anxiety-like behaviour due to stress-induced BDNF reduction in the hippocampus [70]. In case of human studies, also a similar trend was observed in case of the Val66Met SNP [87]. Various mouse models characterized by reduced anxiety-like behaviour have been developed, however the mechanism underlying this phenotype has been challenging to explain. For instance, previous pharmacological investigations into the role of the V1aR in anxiety have yielded a contradictory and inconsistent collection of data [81]. Furthermore, CaMKIV when located in the nucleus, phosphorylates cAMP response element binding (CREB). The reduced anxiety-like behaviour in CaMKIV KO mice contradicts the reported increase in anxiety-like behaviour in CREB-deficient mice, while CREM (CREB-related transcription factor) mutant mice were hyperactive in the open field but displayed reduced anxiety in the elevated plus maze. Moreover CaMKIV mice had a down-regulation

of the oxytocin and the vasopressin genes. The decreased vasopressin expression is in line with the phenotype observed in V1aR phenotype, while the decreased expression of oxytocin counteracts the accumulating evidence suggesting that oxytocin possesses anxiolytic properties. The neuronal circuitry involved in anxiety is known to involve the amygdala and hypothalamic areas, but as the data exposed indicates, the specific signalling pathways involved in the regulation of anxiety-like behaviour is unknown. Regarding that CamKIV and BDNF are involved in the regulation of MAPK signalling pathway, the phenotype the Kidins220 cKO mice display is probably caused by a defective activation this pathway. Nonetheless further studies need to be conducted in order to clarify the specific involvement of Kidins220 in this anxiolytic effect.

## III.II Brain morphology: hydrocephalus

The brain morphology analysis of the Kidins220 cKO mice revealed a notable enlargement of the lateral and the third ventricles in the absence of cell death, disruption of cortical layers and alteration of hippocampal volume. Intriguingly, cKO mice are physically identical to WT, so they do not display the typical cranial deformities that are usually associated with hydrocephalus. Moreover, the hippocampal and overall gross brain volume are comparable between WT and cKO mice. When the enlargement of ventricles begins during childhood, the cranial deformities occur, given that the complete cranial suture closure takes place between P7 and P12 [88]. In contrast, when the ventricle dilatation occurs in young adulthood or after, no deformities in head shape are observed. It is probable that the absence of cranial deformities in cKO is due to the timing of the Kidins220 ablation (P14). Although there is no statistical difference in the brain ventricle volume of the Kidins220$^{lox/lox}$ mice compared to the Kidins220$^{+/+}$ mice, a tendency towards enlargement and a high variability across individuals is visible. Therefore the m6 isoform is possibly relevant in the maintenance of brain ventricles as well. This phenotype is strongly conserved across species, as the SINO syndrome in humans, which is caused by the expression of *loss-of-function* variants of Kidins220, has hydrocephalus as one

of its main symptoms. It is in fact clear the crucial role Kidins220 has on the development or maintenance of healthy-size brain ventricles, but the mechanism involved is yet to be unraveled. Indeed, the fact that these pathological manifestations of the SINO syndrome may be generated through a *loss-of-function* mechanism, whereby the truncated variant cannot fulfill the roles of the full-length protein. However, the truncated variants identified in the three patients are similar to the Kidins220 isoform expressed during adulthood. This points towards a *gain-of-function* effect, as these isoforms are expressed at a developmental stage when they are usually not present. Altogether, the pathophysiology of the SINO syndrome is presently unknown and can be only speculated upon, and it will be the focus of our future investigations.

### III.III WT(+/Cre) mice phenotype differes from Kidins220$^{+/+}$ mice

The data on Cre expressing animals reveal an impact of Cre on some behavioural tests. WT(+/Cre) mice are characterized by increased anxiety-like phenotype in the open field and reduced freezing behaviour during the novel context + cue trial of fear conditioning test, in absence of a defective auditory fear conditioning. In addition WT (+/Cre) display less social interaction in the 'social habituation test' in absence of impaired social discrimination. Albeit we did not address this issue, we believe also some morphological properties of brain neurons, such as dendritic arborization or spine/synapse formation, may be affected by Cre expression. In addition, the impact of Cre and its expression levels are bound to be very different depending on the promoter controlling its expression, and on the genetic background of the colony. The mechanisms underlying the observed alterations were not further investigated since it would go beyond the scope of this project. However, this indicates that Cre-expressing mice should not be considered as wild type, but always be taken as control when a conditional knockout colony is under study. Moreover, the fact that WT(+/Cre) and Kidins220$^{+/+}$ mice are born in different litters should not be ignored. The importance of maternal care and sibling interaction is known to be crucial for behaviour and cognition in adult mice (and humans). As a consequence, Cre expressing mice are the most appropriate controls for cKO because of the putative

effects of Cre in the mice physiology, but also because of the environmental effects during embryonic stage and childhood. That being said, Cre expressing mice are not to be considered wildtype, but control mice.

# IV Future perspectives

## IV.I Rescue experiment

As described in the introduction, Kidins220 interacts with all other neurotrophin receptors, and in the brain, this is particularly relevant for TrkB. It is already known that brain slices from cKO mice have lower basal levels of phosphorylated MAPK and phosphorylated TrkB receptor, indicating lower basal levels of activation of the MAPK pathway (**Figure 6, Introduction**). With the objective of gaining further insights on the molecular pathways involved in the behavioural phenotype seen in the cKO mice, a phenotype rescue experiment has been initiated. The possible involvement of BDNF signalling in the behavioural defects is being investigated by treating the mice with the BDNF-mimetic drug DHF. DHF is known to cross the blood-brain barrier upon oral ingestion and induce BDNF/TrkB signalling [89]. DHF is part of a group of small molecules widely used for the TrkB stimulation in vivo. However, the exact mechanism by which DHF elicits this effect is presently not known and object of debate since many of those molecules have failed to show TrkB phosphorylation and ERK pathway activation in vitro. Nevertheless, a considerable amount of literature shows DHF-induced activation of TrkB signalling *in vivo*. One current interpretation of the published data is that it is not the DHF molecule *per se* that acts as a BDNF-mimetic drug, but rather the metabolites originated upon DHF digestion [90]. The treatment protocol was done following the indications described by Parrini and colleagues [91] (details are provided in the **Materials and Methods** section) diluting DHF in the mice drinking water. The solution intake of both vehicle and treatment groups were monitored, as well as the weight of the animals. All the treated mice were housed in couples.

We considered three experimental groups: (i) WT and (ii) cKO treated with vehicle solution (controls), and (iii) cKO treated with DHF solution. The inclusion of a 4th group was considered, i.e. WT treated with DHF, however, it is reported that DHF failed to induce significant changes in TrkB signalling in wild type animals [91], therefore this group has not been included in the experimental procedure. The behavioural

tests performed on the treated mice were the ones where an impaired phenotype was previously observed in cKO, i.e. fear conditioning, open field, elevated plus maze, social habituation / dis-habituation, and olfactory memory. The experiments are still in progress and only a limited number of animals have been tested, therefore no statistical analysis has been performed yet. Amongst those tests, the results of the olfactory habituation are the most promising, and are shown in **Figure 19 A**. The behaviour of cKO-DHF animals, in fact, was more comparable to the WT-vehicle than to the cKO-vehicle mice, being the behaviour of the two vehicle groups comparable to the previously obtained results. In addition, females cKO-DHF seemed to be more affected by the treatment than the males, as their behaviour was indistinguishable from that of the WT-vehicle mice (**Figure 19 B**). Consequently, there probably is a partial rescue of the phenotype by elevating TrkB signalling in vivo.

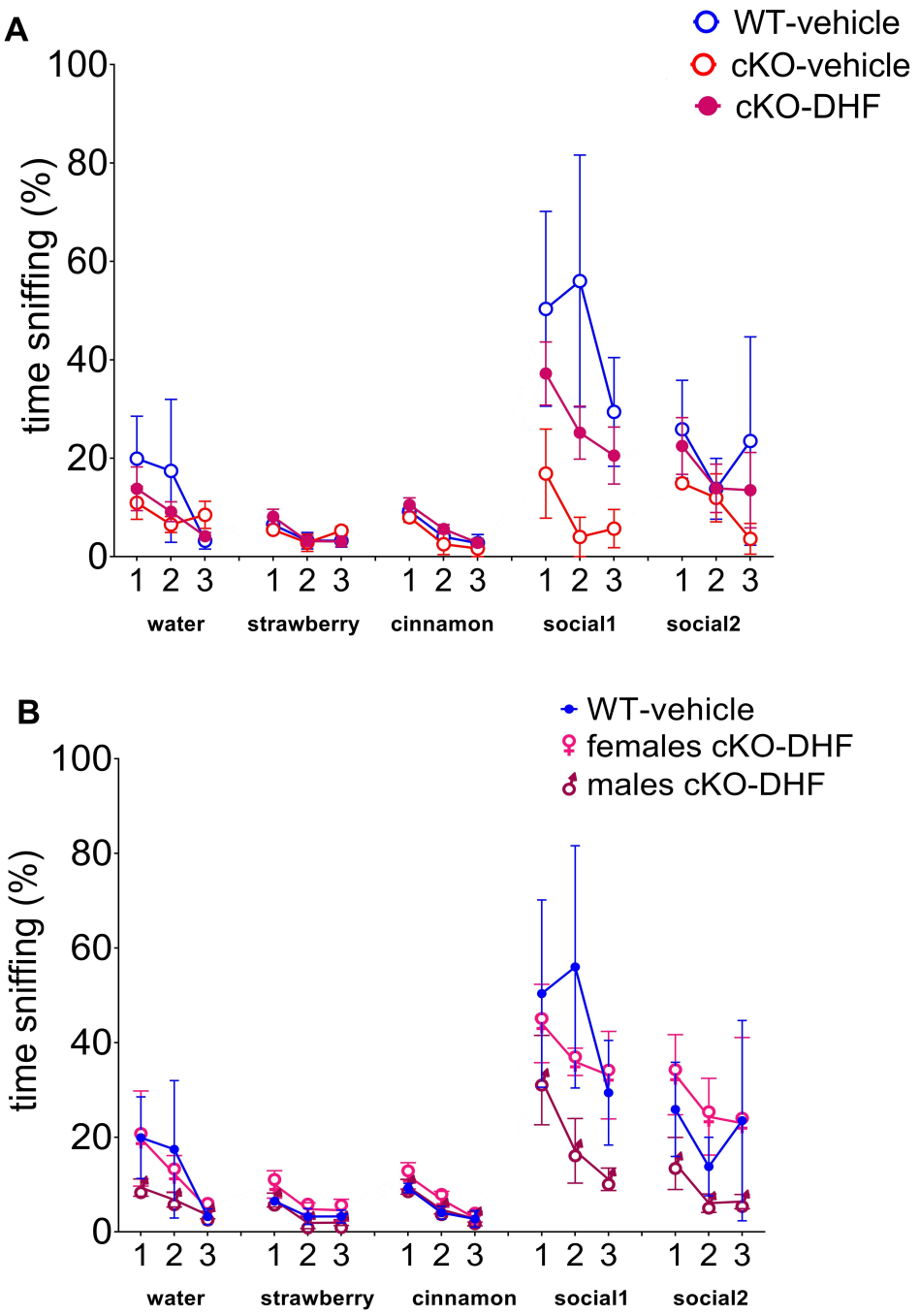


Figure 19. **A. Olfactory ability.** Results for WT-vehicle (n = 9, blue), cKO-vehicle (n = 2, red) and cKO-DHF (n = 7, magenta, full circles) animals are shown. The olfactory habituation results are expressed as the % time each mouse spent sniffing the cotton-swab in the presence of different smells, as indicated. **B.** Results for WT-vehicle (n = 9, blue), cKO-DHF males (n = 4, dark magenta) and cKO-DHF females (n = 3, pink) mice. The results are expressed as means.e.m. in both panels.

## IV.II Social behaviour impairment

cKO mice have impairment in social odour discrimination and conspecific discrimination, which is a phenotype observed in oxytocin-deficient mice. In addition, oxytocin has lately been a widely chosen target for the study of social deficits in ASD and schizophrenia. Given the scaffolding function of Kidins220, it is probable that it serves as a converging element between BDNF and oxytocin signalling pathways, leading to the observed phenotypes in Kidins220 cKO and Kidins220$^{lox/lox}$ mice. Oxytocin expression quantification has proven to be challenging, so its involvement in Kidins220 role in social behaviour will be determined by gene expression of oxytocin and its receptors. Not only oxytocin has been strongly involved in social behaviour, when it comes to determining relevant brain areas, but CA2 has also been related to social memory [92]. The planned assessment of gene expression is intended to be complemented by electrophysiological studies of CA2 connectivity and excitatory/inhibitory balance in Kidins220 cKO mice. Following this research path, it would be useful to observe the excitatory/inhibitory balance of the VNO and its connectivity with cortical encoding areas as the piriform cortex. Given the involvement of BDNF in the processing of social odour encoding and the hidrocephalus detected in the cKO, the rostral migratory stream could be involved in this phenotype. The subventricular zone (SVZ) is a known source of neuronal progenitors in adult rodents that provides the olfactory bulb with new neurons. BDNF is a growth factor with key involvement, shared with Kidins220, in neuronal progenitors migration maturation [93], and Kidins220 may be part of this signalling system. Moreover, since the SVZ lays immediately adjacent to the ventricles, the presence of hydrocephalus may cause physical damage to the cells in that zone. We plan to perform a series of histochemical and biochemical studies in order to assess the possible relation between BDNF signalling and the rostral migratory stream, ventricle enlargement and the impaired social odour recognition in cKO mice.

## IV.III Sexual dimorphism

Different phenotypes in males and females in contextual memory and social olfactory discrimination rescue indicates a putative distinctive function of Kidins220, related to estrogenic and androgenic signalling. The relevant involvement of sex hormones in learning and memory and the endogenous synthesis if these compounds in brain areas as the hippocampus indicate a research line to be explored. ASD have a 5:1 ratio of incidence on boys:girls in humans (autism.org.uk) and schizophrenia onsets in an earlier age in men [94]. Therefore sex dimorphism is a relevant issue to study more importantly when investigating the role of a documented genetic risk factor for these psychiatric disorders as Kidins220. That is why estrogen signalling paired to downstream BDNF and Kidins220 activation will be assessed by quantifying protein expression and phosphorylation of downstream BDNF effectors. In addition, gene expression will be determined for DHF-treated mice.

## IV.IV Neuronal morphology

The hypothesised defective BDNF signalling in Kidins220 cKO mice could be responsible for the observed decreasing dendritic arborisation in the motor cortex and the differential pattern in dendritic arborisation in the dentate gyrus of the hippocampus. Dendritic spine quantification and morphological analysis will be done in cKO and DHF treated cKO not only in the motor cortex and the dentate gyrus but also in the other affected areas as CA2-CA3 areas of the hippocampus and the VNO. Understanding the molecular and physiological role of Kidins220 in the adult cortico-hippocampal circuits will provide a potential research path towards a deeper understanding of symptomatology in psychiatric disorders as ASD and schizophrenia. This would contribute to earlier diagnosis and more importantly intervention upon the onset of these disorders.

# V Materials and methods

## V.I Animals

In this study, three different mouse lines were used. The Kidins220lox colony and the CaMKIICre colonies were used to generate the Kidins220 cKO mice. The Kidins220lox colony was obtained from Dr G. Shiavo (UCL London, UK) and the CaMKIICre mouse line was bought from Jackson Laboratories (Maine, USA) [#B6.Cg-Tg(Camk2a-cre)T29-1Stl/J]. All the animal colonies used were on the C57BL/6 background. All procedures were approved by the Italian Ministry of Health (permit n° 254/2015-PR and permit n° 474/2018-PR) and strictly adhere to the recommendations in the Guide for the Care and Use of Laboratory Animals of the National Institutes of Health.

### V.I.1 Crossing plan

In order to analyze the role of Kidins220 in the adult mouse brain, a new conditional knockout mouse line was generated by crossing the Kidins220-lox animals with transgenic mice that express Cre recombinase under the control of the Calmodulin dependent Protein Kinase II (CaMKII) promoter. This promoter was selected because it drives the expression of Cre only in the excitatory forebrain starting from the second postnatal week, thus circumventing developmental defects in the nervous and cardiovascular systems. This line was established as an essential tool to investigate any abnormalities arising in the adult brain due to the lack of Kidins220, as well as to understand the role of Kidins220 in the formation and maintenance of the cortico-hippocampal circuits. A 4- step crossing plan was designed to obtain the cKO animals, as shown in **Figure 20**.

### V.I.2 Genotyping of animals

All animals were individually genotyped with the polymerase-chain reaction (PCR) technique for the floxed allele, for the Cre allele and for the tissue-specific activation of Cre. Genomic DNA was isolated from tail or ear snips of young mouse pups for determining their genotype. This tissue was lysed rapidly by incubating it in 50

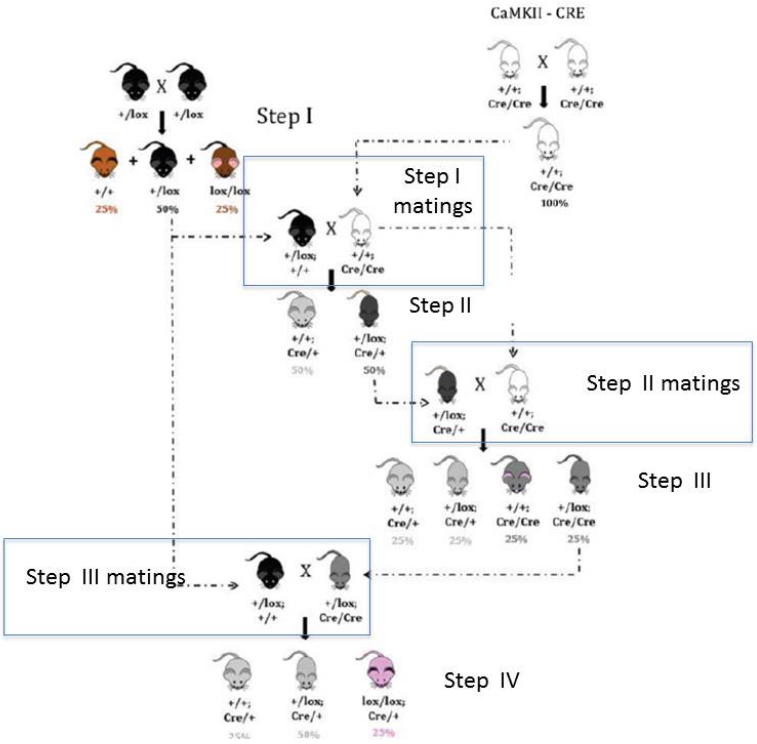


Figure 20. **Crossing plan.** Kidins220-lox animals are in black, CaMKIICre animals in white, all the intermediate genotypes are in grey, cKO animals are depicted in pink. The expected percentage of pups of each genotype is indicated.

mM sodium hydroxide (NaOH) at 98°C for 50 min. Kidins220$^{lox/lox}$ and CaMKIICre genotyping PCRs were performed using the GoTaq Green PCR Master Mix (M712, Promega). It is a ready-to-use solution that facilitates the direct loading of the PCR products onto agarose gels. It contains Taq DNA Polymerase, coloured dyes, $MgCl_2$ and dNTPs. The genomic DNA amplified by the PCRs was run on a 2% agarose gel (prepared by dissolving 2% agarose in Tris Acetate-EDTA (TAE) Buffer (Sigma-Aldrich) and SyverSafe at a final concentration of 0.1 $\mu$g/mL). The PCR samples were loaded directly onto the agarose gel and electrophoresed at 80 V in TAE Buffer. 5 ng of the genomic DNA were used for performing a quantitative PCR using an ABI 7500 and the TaqManR Universal PCR Master Mix, no AmpEraseR UNG (ThermoFisher Scientific). A fluorophore-quencher combination (as recommended by the Jackson Laboratory) was used to determine if the Cre transgene was expressed in

Table 1. **List of primers**

| Primer Name | | Sequence 5' to 3' |
|---|---|---|
| Kidins220 Primers | Long | GAGCACAGACTTCTCTTATGG |
| | Flox | GCGTTTCTAGCATACACATG |
| | Splice | CAGATGGCTGTGAACCACCGTTTAAAC |
| CRE Primers | Transgene Fw | GCGGTCTGGCAGTAAAAACTATC |
| | Transgene Rv | GTGAAACAGCATTGCTGTCACTT |
| | Internal Positive Control Fw | CTAGGCCACAGAATTGAAAGATCT |
| | Internal Postitive Control Rv | GTAGGTGGAAATTCTAGCATCATCC |
| CRE qRT-PCR Primers | Tg Probe | AACATGCTTCATCGTCGGTCCGG |
| | Transgene Fw | GCGGTCTGGCAGTAAAAACTATC |
| | Transgene Rv | GTGAAACAGCATTGCTGTCACTT |
| | Internal Positive Control Fw | CACGTGGGCTCCAGCATT |
| | Internal Positive Control Rv | TCACCAGTCATTTCTGCCTTTG |
| | IC Probe | CCAATGGTCGGGCACTGCTCAA |

heterozygosity or homozygosity.

## V.II behavioural experiments

The mice tested were 3-5 months old. The animals were housed with minimum 2 and maximum 6 mice per cage, in a climate-controlled animal facility (22°C±2°C) and maintained in a 12 h light/dark cycle. Even though specifically cKO and WT and Kidins220$^{+/+}$ and Kidins220$^{lox/lox}$ mice were tested, the heterozygous for both genotypes were kept in the cages to avoid changes in housing conditions. Food and water were available *ad libitum*. 1 h habituation in a third room was mandatory before performing all tests. Males and females were tested separately in all tests, cleaning the apparatus with 70% ethanol between different animals as well as different trials. The animals were handled by the experimenter the week prior to the tests, during 3-5 days (the mice were handled until fear reactions as jumping, defecating or urinating during handling were extinguished) 5 minutes per animal. Experimenters were blind

to the mouse genotype during testing and behavioural scoring.

### V.II.1 Fear Conditioning

The *Any-maze software* was used for recording and storing the videos. The experimenter scored the freezing behaviour manually.

**Conditioning phase:** A 40 cm x 40 cm closed chamber with transparent walls and an electrical grid as a floor is used for the test where the animal is situated. The animals were tested for 510s. During this session, the cue (i.e. the sound of 75 dB of volume and 4 kHz of frequency) was followed by the aversive stimulus (i.e. an electrical foot shock of 0.7 mA of intensity), which constituted a trial of 30 s followed by an inter-trial interval (ITI) of 90 s. The animals were conditioned with 3 consecutive trials after 2min of habituation to the conditioning chamber using the*TSE Multiconditioning System, FCS v9.02 or Shuttle 4.07.*

**Context phase:** 24 h later the animals were tested in the conditioning chamber for 5 min without the tone or foot shock. The environmental conditions were kept identical to the training session.

**Novel context phase:** 1 h post context testing, the animals were tested in a novel environment for 6 min. The animals were in 40cm x 40cm chamber of black opaque walls, with the grid floor covered with a grey plastic cover and a filter paper embedded in 20$\mu$l of apricot essential oil. The animals were exposed to the same cue played during the conditioning phase, during 2 min after a 2 min habituation to the novel context. After the cue, the animals were kept 2 min in the novel chamber.

### V.II.2 Open field

The basic locomotor activity was tested in the open field test by placing each animal in a large square empty open arena (45 cm X 45 cm X 45 cm) surrounded by non-transparent sides for 30-60 min under red light. The mice were situated in the centre

of the maze at the beginning of the test. An overhead camera recorded the animals and the video was stored, tracked and analysed by the Stoelting ANY-maze software (U.S.A.). Stoelting ANY-maze software (U.S.A.) calculated the total distance covered and average speed. A square 20 cm X 20 cm zone was determined in the centre of the arena (marked as the central zone). The same software also calculated the time spent by each animal in this zone.

### V.II.3 Elevated Plus maze

The elevated plus maze is a plus shaped maze with four equal sized arms (30 cm X 15 cm), two of which lack sides, while the other two are walled (15 cm high). The maze is elevated by 70 cm from the ground level. The test was performed under red light and during the experiment the experimenter was present in the room. The mouse began the test being situated in the middle of the cross. An overhead camera recorded the test. The *Stoelting ANY-maze* software was used to score the video and calculate the number of entrances into each arm and the time spent in each arm.

### V.II.4 Social habituation

The social habituation test was performed as similarly reported previously [95] in a transparent plastic cage with filter lid and $\sim$ 1cm of bedding. The experiment consisted of 5 trials that lasted 5 min with inter-trial-intervals of 2 min. During the 4 first trials the test mouse (the animal being tested) was faced with a stimulus mouse (which was always WT or Kidins220$^{+/+}$) and they were free to interact. During the 5$^{th}$ trial the stimulus mouse was a different one (still with the same genotype as the anterior stimulus mouse). A camera situated beside the cage recorded the test. The social habituation was assessed by manually determining the social interaction (% time the test mouse spent sniffing the stimulus mouse).

### V.II.5 Social memory

The social memory test was performed in a transparent cage with filter lid and $\sim$1 cm of bedding. The test mouse (the mouse monitored for assessing its social behaviour) was placed in the cage 1 h before the test for habituation. After that, the stimulus mouse was introduced to the cage and the animals were free to interact during 5min. After that, the stimulus mouse was extracted from the cage and the test mouse remained in the testing cage during the 1 h inter-trial-interval. Then, the stimulus mouse for the $2^{nd}$ trial was introduced to the cage for 5 min of social interaction. When the stimulus mouse on the second trial was different from the first stimulus mouse, it was selected from a different cage. Some of the social interaction trials derived in violent interactions. These trials were not accounted for in the results. Most of the test animals were tested in the two modalities of the experiment (the second trial with the same stimulus mouse or with a different one). When testing the same test mouse, the two parts of the experiment where performed 24 hours apart.

### V.II.6 Olfactory memory

The olfactory habituation test was performed following the protocol described in the paper from Yang, M. and Crawley, N. in 2009 [96]. The non-social odours presented to the mice were cinnamon and strawberry essential oils. The cotton tip was dipped during 2 s and then let dry during 5 s. The test was performed in 210E Tecniplast cage (35.5 x 23.5 x 19 cm) lightly illuminated (5$\pm$1 lux). The experimenter was in the room throughout the entire test registering with a digital timer the sniffing behaviour during each 2 min trial. Social odour stimuli were acquired by swiping the cage bottom from mice matched in genotype and gender to the tested mice.

### V.II.7 Pre-pulse inhibition and acoustic startle response

Acoustic startle response and prepulse inhibition (PPI) were measured using four TSE Multiconditioning System, FCS v9.02 or Shuttle 4.07, following the protocol reported in [97]. Startle and PPI experiment test sessions began by placing the mouse in the metallic chamber (5cm x 5cm x 5cm). During the startle response test

each subject received 36 trials over a 9 min session. Each stimulus was 40 ms and presented four times at pseudorandom order and the ITI was 10-20 ms. The TSE System software registered the startle amplitude, the mean amplitude was used as dependent variable. During the PPI test the trial types were presented randomly within each block. The ITI were 10-20 s Prepulse tones were at 20 ms and each trial was a 40 ms, 120 dB sound.

## V.III Histology experiments

### V.III.1 Brain ventricle volume measurements

**Brain extraction:** The mice were anesthetised with a lethal dose of isofluorane and perfused transcardially with approximately 15$\pm$5 ml of a 4% solution of paraformaldheide (PFA) in phosphate-buffered saline (PBS) 1x. Once the tissue fixation was assessed by the level of stiffening of the tail and jaw of the animal, the brain was extracted. All the brains were incubated at 4$^{\circ}$C in 4% PFA during 24 h post-extraction and then transferred to a 20% sucrose solution in MilliQ water. The brains were only sliced when they sank in the sucrose solution to the bottom of the container.

**Brain slicing:** The perfused brains were sliced with a vibrating microtome (model 5100MZ Campbel Instruments Ltd., UK) at a frequency of 80 Hz, 0.5mm amplitude and 180 $\mu$m of thickness while submerged in a 6% sucrose solution. The brain slices comprehending from the frontal origin of the lateral ventricles to the dorsal hippocampus were mounted in glass slides. After letting the brain slices dry slightly to ensure adherence to the slides, they were covered with mounting medium Moviol and covered with 1.5mm glass cover.

**Brain imaging and analysis:** Brain slices were imaged with a Nikon Leica microscope (Nicon Eclipse-DS-Qi2) with the 4x objective in a scale of 2.2 $\mu$m/pixel. The volume of the ventricles was calculated from the area of the ventricles in each brain slice. The area was obtained with ImageJ and then the volume was extracted by multiplying each area to the 180 $\mu$m of thickness of

each brain slice. The total volume of each ventricle is the sum of the volumes from all the brain slices of an animal. The results are expressed as the mean of the brain ventricle volumes of all the animals from each genotype.

### V.III.2 Sholl analysis

**Golgi Staining:** 3 months old animals were perfused transcardially with saline (0,9% NaCl in deionized water (DW)). Then the brains were incubated in Golgi-Cox solution for 39 h at 37°C. After that period, they were incubated in a sucrose solution (20% sucrose in DW) for minimum 2 days at 4°C. Brains were sliced with a vibrating microtome while submerged in a 6% sucrose solution while maintaining the room as dark as possible. The slices were of 150-200 $\mu$m of thickness and mounted on 2% gelatin-coated glass slides. After leaving the brain slices dry, the Golgi-Cox staining was developed using this sequence:

1. DW 5 min + agitation (2x)
2. 33% ammonium hydroxyde 30min
3. DW 5 min + agitation (2x)
4. Sodium thiosulfate 1% in DW 30min
5. DW 5min + agitation (2x)
6. 50% EtOH 1min
7. 70% EtOH 1min
8. 95% EtOH 1min
9. 100% EtOH 5min (2x)
10. Solution X (1/3 chloroform + 1/3 xylene + 1/3EtOH) 15 min
11. Xylene 15 min
12. Coverslip with Moviol

**Golgi-Cox solution preparation:** 5 volumes of solution A (5% w/v potassium dichromate ($K_2Cr_2O_7$) were mixed with 5 volumes of solution B (5gr/100ml DW Mercuric Chloride ($HgCl_2$) and this mix was stirred for 30 min 4 volumes of solution C (5% w/v potassium chromate ($K_2CrO_4$) were mixed with 10 volumes of DW and gently stirred. Then, solution C was added to the mix A+B slowly and the Golgi-Cox solution (A+B+C) was stirred for 30 min in a glass bottle in the dark and incubated for 5 days. Before using the solution, it was filtered (cellulose acetate filter 0.45$\mu$m, Sartorius Stedim Biotech GmbH) into a new bottle.

**Imaging of slices:** The Golgi-stained brain slices were imaged at 4X magnification (using an Olympus BX51 Neurolucida Microscope) to acquire the entire slice and the specific regions in the motor and sensory cortices were imaged at 10X magnification. For imaging the granule cells from the dentate gyrus of the hippocampus, neurons were imaged at 40x (using a Leica SP8 Confocal Microscope). Single neurons were analyzed using the Advanced Sholl Analysis ImageJ Plugin and the Simple Neurite tracer ImageJ Plugin. Intersections every 5 $\mu$m were counted and plotted in the form of line graphs. The motor and sensory cortex analysis was done on entire neurons as well as separately on the apical and basal processes. The dentate gyrus analysis was done on entire neurons.

## V.IV Rescue experiment

The protocol was performed as detailed previously [91]. All the cages housing 7,8-Dihydroxyflavone (DHF)-treated animals contained 2 animals/cage and the vehicle cages consisted of 4 cages with 3 animals and 2 cages with 2. Animals of different genotypes were mixed in the vehicle-treated cages. The DHF treatment was applied for 4 weeks prior to the behavioural experiments and the week during which the behavioural experiments were performed. Solution intake was monitored every 2 days and changed every 2 days. All the drinking bottles were covered with aluminium foil for avoiding DMSO oxidation.

## V.V Statistical analysis

The statistical analysis is described in the figure legends. All data were tested for normality (D'Agostino & Pearson test) and outliers (ROUT test). For comparing means Student's t-test was used for parametric data and Mann-Whitney test for non-parametric data. 2 way RM-ANOVA test was performed to compare multiple groups with Sidak's *post-hoc* test. Statistical significance was set at P value $< 0.05$, using GraphPad Prism statistical software 7.03. The experimental groups have different sizes because the animals were tested by litters when they reached 2-3 months of age. The amount of cKO, WT, Kidins220$^{lox/lox}$ and Kidins220$^{+/+}$ in each test depends on the number of animals with each genotype in the litters tested.

# Bibliography

[1] T. Iglesias, N. Cabrera-Poch, M. P. Mitchell, T. J. P. Naven, E. Rozengurt, and G. Schiavo, "Identification and cloning of Kidins220, a novel neuronal substrate of protein kinase D," *Journal of Biological Chemistry*, vol. 275, no. 51, pp. 40048–40056, 2000.

[2] H. Kong, J. Boulter, J. L. Weber, C. Lai, and M. V. Chao, "An evolutionarily conserved transmembrane protein that is a novel downstream target of neurotrophin and ephrin receptors.," *The Journal of neuroscience*, vol. 21, no. 1, pp. 176–185, 2001.

[3] A. M. Higuero, L. Sánchez-Ruiloba, L. E. Doglio, F. Portillo, J. Abad-Rodríguez, C. G. Dotti, and T. Iglesias, "Kidins220/ARMS modulates the activity of microtubule-regulating proteins and controls neuronal polarity and development," *Journal of Biological Chemistry*, vol. 285, no. 2, pp. 1343–1357, 2010.

[4] S. H. Wu, J. C. Arévalo, F. Sarti, L. Tessarollo, W.-B. Gan, and M. V. Chao, "Ankyrin Repeat-rich Membrane Spanning/Kidins220 protein regulates dendritic branching and spine stability in vivo.," *Developmental neurobiology*, vol. 69, no. 9, pp. 547–57, 2009.

[5] J. Li, A. Mahajan, and M.-D. Tsai, "Ankyrin Repeat: A Unique Motif Mediating ProteinProtein Interactions," *Biochemistry*, vol. 45, no. 51, pp. 15168–15178, 2006.

[6] V. E. Neubrand, C. Thomas, S. Schmidt, A. Debant, and G. Schiavo, “Kidins220/ARMS regulates Rac1-dependent neurite outgrowth by direct interaction with the RhoGEF Trio,” *Journal of Cell Science*, vol. 123, no. 12, 2010.

[7] R. Palenzuela, Y. Gutiérrez, J. E. Draffin, A. Lario, M. Benoist, and J. A. Esteban, “MAP1B Light Chain Modulates Synaptic Transmission via AMPA Receptor Intracellular Trapping,” *The Journal of Neuroscience*, vol. 37, no. 41, pp. 9945 LP – 9963, 2017.

[8] A. M. Higuero, L. Sánchez-Ruiloba, L. E. Doglio, F. Portillo, J. Abad-Rodríguez, C. G. Dotti, and T. Iglesias, “Kidins220/ARMS modulates the activity of microtubule-regulating proteins and controls neuronal polarity and development.,” *The Journal of biological chemistry*, vol. 285, no. 2, pp. 1343–1357, 2010.

[9] A. M. Higuero, L. Sánchez-Ruiloba, L. E. Doglio, F. Portillo, J. Abad-Rodríguez, C. G. Dotti, and T. Iglesias, “Kidins220/ARMS modulates the activity of microtubule-regulating proteins and controls neuronal polarity and development.,” *The Journal of biological chemistry*, vol. 285, no. 2, pp. 1343–57, 2010.

[10] J. C. Arévalo, H. Yano, K. K. Teng, and M. V. Chao, “A unique pathway for sustained neurotrophin signaling through an ankyrin-rich membrane-spanning protein.,” *The EMBO journal*, vol. 23, pp. 2358–2368, jun 2004.

[11] S. López-Benito, J. Sánchez-Sánchez, V. Brito, L. Calvo, S. Lisa, M. Torres-Valle, M. E. Palko, C. Vicente-García, S. Fernández-Fernández, J. P. Bolaños, S. Ginés, L. Tessarollo, and J. C. Arévalo, “Regulation of BDNF release by ARMS/Kidins220 through modulation of Synaptotagmin-IV levels,” *The Journal of Neuroscience*, pp. 1653–17, 2018.

[12] J. C. Arévalo, S. H. Wu, T. Takahashi, H. Zhang, T. Yu, H. Yano, T. A. Milner, L. Tessarollo, I. Ninan, O. Arancio, and M. V. Chao, “The ARMS/Kidins220 scaffold protein modulates synaptic transmission,” *Molecular and Cellular Neuroscience*, vol. 45, no. 2, pp. 92–100, 2010.

[13] J. C. Arévalo, D. B. Pereira, H. Yano, K. K. Teng, and M. V. Chao, "Identification of a switch in neurotrophin signaling by selective tyrosine phosphorylation," *Journal of Biological Chemistry*, vol. 281, no. 2, pp. 1001–1007, 2006.

[14] W. Guo, G. Nagappan, and B. Lu, "Differential effects of transient and sustained activation of BDNF-TrkB signaling," *Developmental Neurobiology*, vol. 78, no. 7, pp. 647–659, 2018.

[15] S. Hisata, T. Sakisaka, T. Baba, T. Yamada, K. Aoki, M. Matsuda, and Y. Takai, "Rap1-PDZ-GEF1 interacts with a neurotrophin receptor at late endosomes, leading to sustained activation of Rap1 and ERK and neurite outgrowth," *Journal of Cell Biology*, vol. 178, no. 5, pp. 843–860, 2007.

[16] A. Bracale,* F. Cesca,* V. E. Neubrand,* T. P. Newsome, M. Way and G. Schiavo*, "Kidins220/ARMS Is Transported by a Kinesin-1based Mechanism Likely to be Involved in Neuronal Differentiation," *Molecular Biology of the Cell*, vol. 18, no. 4, pp. 142–152, 2007.

[17] M. B. Kennedy, "Origin of PDZ (DHR, GLGF) domains," *Trends in Biochemical Sciences*, vol. 20, no. 9, p. 350, 1995.

[18] S. Luo, Y. Chen, K. O. Lai, J. C. Arévalo, S. C. Froehner, M. E. Adams, M. V. Chao, and N. Y. Ip, "$\alpha$-syntrophin regulates ARMS localization at the neuromuscular junction and enhances EphA4 signaling in an ARMS-dependent manner," *Journal of Cell Biology*, vol. 169, no. 5, pp. 813–824, 2005.

[19] M. Andreazzoli, G. Gestri, E. Landi, B. D'Orsi, M. Barilari, A. Iervolino, M. Vitiello, S. W. Wilson, and L. Dente, "Kidins220/ARMS interacts with Pdzrn3, a protein containing multiple binding domains," *Biochimie*, vol. 94, no. 9, pp. 2054–2057, 2012.

[20] C. López-Menéndez, S. Gascón, M. Sobrado, O. G. Vidaurre, A. M. Higuero, Á. Rodríguez-Peña, T. Iglesias, and M. Díaz-Guerra, "Kidins220/ARMS downregulation by excitotoxic activation of NMDARs reveals its involvement in neu-

ronal survival and death pathways," *Journal of Cell Science*, vol. 122, no. 19, 2009.

[21] F. Steinberg, M. Gallon, M. Winfield, E. C. Thomas, A. J. Bell, K. J. Heesom, J. M. Tavaré, and P. J. Cullen, "A global analysis of SNX27-retromer assembly and cargo specificity reveals a function in glucose and metal ion transport," *Nature Cell Biology*, vol. 15, no. 5, pp. 461–471, 2013.

[22] J. LIU and A. LIN, "Role of JNK activation in apoptosis: A double-edged sword," *Cell Research*, vol. 15, p. 36, 2005.

[23] M. Hamanoue, G. Middleton, S. Wyatt, E. Jaffray, R. T. Hay, and A. M. Davies, "p75-Mediated NF-$\kappa$B Activation Enhances the Survival Response of Developing Sensory Neurons to Nerve Growth Factor," *Molecular and Cellular Neuroscience*, vol. 14, no. 1, pp. 28–40, 1999.

[24] G. Middleton, M. Hamanoue, Y. Enokido, S. Wyatt, D. Pennica, E. Jaffray, R. T. Hay, and A. M. Davies, "Cytokine-Induced Nuclear Factor Kappa B Activation Promotes the Survival of Developing Neurons," *The Journal of Cell Biology*, vol. 148, no. 2, pp. 325 LP – 332, 2000.

[25] E. Rozengurt, "Protein Kinase D Signaling: Multiple Biological Functions in Health and Disease," *Physiology*, vol. 26, no. 1, pp. 23–33, 2011.

[26] N. Cabrera-Poch, L. Sánchez-Ruiloba, M. Rodríguez-Martínez, and T. Iglesias, "Lipid raft disruption triggers protein kinase C and Src-dependent protein kinase D activation and Kidins220 phosphorylation in neuronal cells," *Journal of Biological Chemistry*, vol. 279, no. 27, pp. 28592–28602, 2004.

[27] G. J. Fiala, I. Janowska, F. Prutek, E. Hobeika, A. Satapathy, A. Sprenger, T. Plum, M. Seidl, J. Dengjel, M. Reth, F. Cesca, T. Brummer, S. Minguet, and W. W. Schamel, "Kidins220/ARMS binds to the B cell antigen receptor and regulates B cell development and activation," *The Journal of Experimental Medicine*, vol. 212, no. 10, pp. 1693–1708, 2015.

[28] R. M. Jean-Mairet, C. López-Menéndez, L. Sánchez-Ruiloba, S. Sacristán, M. Rodríguez-Martínez, L. Riol-Blanco, P. Sánchez-Mateos, F. Sánchez-Madrid, J. L. Rodríguez-Fernández, M. R. Campanero, and T. Iglesias, "The neuronal protein Kidins220/ARMS associates with ICAM-3 and other uropod components and regulates T-cell motility.," *European journal of immunology*, vol. 41, no. 4, pp. 1035–46, 2011.

[29] L. Riol-Blanco, T. Iglesias, N. Sánchez-Sánchez, G. de la Rosa, L. Sánchez-Ruiloba, N. Cabrera-Poch, A. Torres, I. Longo, J. García-Bordas, N. Longo, A. Tejedor, P. Sánchez-Mateos, and J. L. Rodríguez-Fernández, "The neuronal protein Kidins220 localizes in a raft compartment at the leading edge of motile immature dendritic cells," *European Journal of Immunology*, vol. 34, no. 1, pp. 108–118, 2004.

[30] V. B. Singh, A. K. Wooten, J. W. Jackson, S. B. Maggirwar, and M. Kiebala, "Investigating the role of ankyrin-rich membrane spanning protein in human immunodeficiency virus type-1 Tat-induced microglia activation," *Journal of NeuroVirology*, vol. 21, no. 2, pp. 186–198, 2015.

[31] F. Cesca, a. Yabe, B. Spencer-Dene, J. Scholz-Starke, L. Medrihan, C. H. Maden, H. Gerhardt, I. R. Orriss, P. Baldelli, M. Al-Qatari, M. Koltzenburg, R. H. Adams, F. Benfenati, and G. Schiavo, "Kidins220/ARMS mediates the integration of the neurotrophin and VEGF pathways in the vascular and nervous systems.," *Cell death and differentiation*, vol. 19, no. 2, pp. 194–208, 2012.

[32] A. M. Møller, E. M. Füchtbauer, A. Brüel, T. L. Andersen, X. G. Borggaard, N. J. Pavlos, J. S. Thomsen, F. S. Pedersen, J. M. Delaisse, and K. Søe, "Septins are critical regulators of osteoclastic bone resorption," *Scientific Reports*, vol. 8, no. 1, pp. 1–15, 2018.

[33] I. G. Macara, R. Baldarelli, C. M. Field, M. Glotzer, Y. Hayashi, S.-C. Hsu, M. B. Kennedy, M. Kinoshita, M. Longtine, C. Low, L. J. Maltais, L. McKenzie, T. J. Mitchison, T. Nishikawa, M. Noda, E. M. Petty, M. Peifer, J. R. Pringle, P. J. Robinson, D. Roth, S. E. H. Russell, H. Stuhlmann, M. Tanaka, T. Tanaka, W. S.

Trimble, J. Ware, N. J. Zeleznik-Le, B. Zieger, and S. R. Pfeffer, “Mammalian Septins Nomenclature,” *Molecular Biology of the Cell*, vol. 13, no. 12, pp. 4111–4113, 2002.

[34] C. L. Beites, H. Xie, R. Bowser, and W. S. Trimble, “The septin CDCrel-1 binds syntaxin and inhibits exocytosis,” *Nature Neuroscience*, vol. 2, p. 434, 1999.

[35] C. L. BEITES, K. A. CAMPBELL, and W. S. TRIMBLE, “The septin Sept5/CDCrel-1 competes with $\alpha$-SNAP for binding to the SNARE complex,” *Biochemical Journal*, vol. 385, no. 2, pp. 347 LP – 353, 2005.

[36] F. Cesca, A. Satapathy, E. Ferrea, T. Nieus, F. Benfenati, and J. Scholz-Starke, “Functional interaction between the scaffold protein Kidins220/ARMS and neuronal voltage-gated Na+ channels,” *Journal of Biological Chemistry*, vol. 290, no. 29, pp. 18045–18055, 2015.

[37] V. E. Neubrand, F. Cesca, F. Benfenati, and G. Schiavo, “Kidins220/ARMS as a functional mediator of multiple receptor signalling pathways,” *Journal of Cell Science*, vol. 125, no. 8, pp. 1845–1854, 2012.

[38] N. Schmieg, C. Thomas, A. Yabe, D. S. Lynch, and T. Iglesias, “Novel Kidins220 / ARMS Splice Isoforms : Potential Specific Regulators of Neuronal and Cardiovascular Development,” pp. 1–21, 2015.

[39] M. S. Chang, J. C. Arevalo, and M. V. Chao, “Ternary complex with Trk, p75, and an ankyrin-rich membrane spanning protein,” *Journal of Neuroscience Research*, vol. 78, no. 2, pp. 186–192, 2004.

[40] S. Cai, J. Cai, W. G. Jiang, and L. Ye, “Kidins220 and tumour development: Insights into a complexity of cross-talk among signalling pathways (Review),” *International Journal of Molecular Medicine*, vol. 40, no. 4, pp. 965–971, 2017.

[41] Y. H. Liao, S. M. Hsu, H. L. Yang, M. S. Tsai, and P. H. Huang, “Upregulated ankyrin repeat-rich membrane spanning protein contributes to tumour progression in cutaneous melanoma,” *British Journal of Cancer*, vol. 104, no. 6, pp. 982–988, 2011.

[42] D. A. Rogers and N. F. Schor, “Kidins220/ARMS is expressed in neuroblastoma tumors and stabilizes neurotrophic signaling in a human neuroblastoma cell line,” *Pediatric Research*, vol. 74, no. 5, pp. 517–524, 2013.

[43] H. Jung, J.-h. Shin, Y.-s. Park, and M.-s. Chang, “Ankyrin Repeat-Rich Membrane Spanning ( ARMS )/ Kidins220 Scaffold Protein Regulates Neuroblastoma Cell Proliferation through p21,” *Molecules and Cells*, vol. 37, no. 12, pp. 881–887, 2014.

[44] J. N. Hansen, X. Li, Y. G. Zheng, L. T. Lotta, A. Dedhe, and N. F. Schor, “Using Chemistry to Target Neuroblastoma,” *ACS Chemical Neuroscience*, vol. 8, no. 10, pp. 2118–2123, 2017.

[45] D. Carvalho, A. Mackay, L. Bjerke, R. G. Grundy, C. Lopes, R. M. Reis, and C. Jones, “The prognostic role of intragenic copy number breakpoints and identification of novel fusion genes in paediatric high grade glioma,” *Acta Neuropathologica Communications*, vol. 2, no. 1, pp. 1–12, 2014.

[46] C. Ballatore, V. M.-Y. Lee, and J. Q. Trojanowski, “Tau-mediated neurodegeneration in Alzheimer’s disease and related disorders,” *Nature Reviews Neuroscience*, vol. 8, p. 663, 2007.

[47] C. López-menéndez, A. Gamir-morralla, J. Jurado-arjona, A. M. Higuero, M. R. Campanero, I. Ferrer, F. Hernández, J. Ávila, M. Díaz-Guerra, and T. Iglesias, “Kidins220 accumulates with tau in human alzheimer’s disease and related models: Modulation of its calpain-processing by GSK3-beta/PP1 imbalance,” *Human Molecular Genetics*, vol. 22, no. 3, pp. 466–482, 2013.

[48] A. Gamir-Morralla, O. Belbin, J. Fortea, D. Alcolea, I. Ferrer, A. Lleó, and T. Iglesias, “Kidins220 Correlates with Tau in Alzheimer’s Disease Brain and Cerebrospinal Fluid,” *Journal of Alzheimer’s Disease*, vol. 55, no. 4, pp. 1327–1333, 2017.

[49] *Diagnostic and statistical manual of mental disorders : DSM-5*. Fifth edition. Arlington, VA : American Psychiatric Publishing ©, 2013.

[50] S. W. Kong, C. D. Collins, Y. Shimizu-Motohashi, I. A. Holm, M. G. Campbell, I. H. Lee, S. J. Brewster, E. Hanson, H. K. Harris, K. R. Lowe, A. Saada, A. Mora, K. Madison, R. Hundley, J. Egan, J. McCarthy, A. Eran, M. Galdzicki, L. Rappaport, L. M. Kunkel, and I. S. Kohane, "Characteristics and Predictive Value of Blood Transcriptome Signature in Males with Autism Spectrum Disorders," *PLoS ONE*, vol. 7, no. 12, 2012.

[51] D. Pinto, E. Delaby, D. Merico, M. Barbosa, A. Merikangas, L. Klei, B. Thiruvahindrapuram, X. Xu, R. Ziman, Z. Wang, J. A. S. Vorstman, A. Thompson, R. Regan, M. Pilorge, G. Pellecchia, A. T. Pagnamenta, B. Oliveira, C. R. Marshall, T. R. Magalhaes, J. K. Lowe, J. L. Howe, A. J. Griswold, J. Gilbert, E. Duketis, B. A. Dombroski, M. V. De Jonge, M. Cuccaro, E. L. Crawford, C. T. Correia, J. Conroy, I. C. Conceio, A. G. Chiocchetti, J. P. Casey, G. Cai, C. Cabrol, N. Bolshakova, E. Bacchelli, R. Anney, S. Gallinger, M. Cotterchio, G. Casey, L. Zwaigenbaum, K. Wittemeyer, K. Wing, S. Wallace, H. Van Engeland, A. Tryfon, S. Thomson, L. Soorya, B. Roge, W. Roberts, F. Poustka, S. Mouga, N. Minshew, L. A. McInnes, S. G. McGrew, C. Lord, M. Leboyer, A. S. Le Couteur, A. Kolevzon, P. Jimenez Gonzalez, S. Jacob, R. Holt, S. Guter, J. Green, A. Green, C. Gillberg, B. A. Fernandez, F. Duque, R. Delorme, G. Dawson, P. Chaste, C. Cafa, S. Brennan, T. Bourgeron, P. F. Bolton, S. Belte, R. Bernier, G. Baird, A. J. Bailey, E. Anagnostou, J. Almeida, E. M. Wijsman, V. J. Vieland, A. M. Vicente, G. D. Schellenberg, M. Pericak-Vance, A. D. Paterson, J. R. Parr, G. Oliveira, J. I. Nurnberger, A. P. Monaco, E. Maestrini, S. M. Klauck, H. Hakonarson, J. L. Haines, D. H. Geschwind, C. M. Freitag, S. E. Folstein, S. Ennis, H. Coon, A. Battaglia, P. Szatmari, J. S. Sutcliffe, J. Hallmayer, M. Gill, E. H. Cook, J. D. Buxbaum, B. Devlin, L. Gallagher, C. Betancur, and S. W. Scherer, "Convergence of genes and cellular pathways dysregulated in autism spectrum disorders," *American Journal of Human Genetics*, vol. 94, no. 5, pp. 677–694, 2014.

[52] T. M. Kazdoba, P. T. Leach, and J. N. Crawley, "Behavioral phenotypes of genetic mouse models of autism," *Genes, Brain and Behavior*, vol. 15, no. 1, pp. 7–

26, 2015.

[53] J. J. Nadler, S. S. Moy, G. Dold, N. Simmons, A. Perez, N. B. Young, R. P. Barbaro, J. Piven, T. R. Magnuson, and J. N. Crawley, “Automated apparatus for quantitation of social approach behaviors in mice,” *Genes, Brain and Behavior*, vol. 3, no. 5, pp. 303–314, 2004.

[54] H. G. McFarlane, G. K. Kusek, M. Yang, J. L. Phoenix, V. J. Bolivar, and J. N. Crawley, “Autism-like behavioral phenotypes in BTBR T+tf/J mice,” *Genes, Brain and Behavior*, vol. 7, no. 2, pp. 152–163, 2007.

[55] M. L. Scattoni, L. Ricceri, and J. N. Crawley, “Unusual repertoire of vocalizations in adult BTBR T+tf/J mice during three types of social encounters,” *Genes, Brain and Behavior*, vol. 10, no. 1, pp. 44–56, 2011.

[56] L. J. Seidman and A. F. Mirsky, “Evolving Notions of Schizophrenia as a Developmental Neurocognitive Disorder,” *Journal of the International Neuropsychological Society*, vol. 23, no. 9-10, pp. 881–892, 2017.

[57] T. M. Kranz, R. R. Goetz, J. Walsh-Messinger, D. Goetz, D. Antonius, I. Dolgalev, A. Heguy, M. Seandel, D. Malaspina, and M. V. Chao, “Rare variants in the neurotrophin signaling pathway implicated in schizophrenia risk,” *Schizophrenia Research*, vol. 168, no. 1-2, pp. 421–428, 2015.

[58] D. Malaspina, T. M. Kranz, A. Heguy, S. Harroch, R. Mazgaj, K. Rothman, A. Berns, S. Hasan, D. Antonius, R. Goetz, M. Lazar, M. V. Chao, and O. Gonen, “Prefrontal neuronal integrity predicts symptoms and cognition in schizophrenia and is sensitive to genetic heterogeneity,” *Schizophrenia Research*, vol. 172, no. 1-3, pp. 94–100, 2016.

[59] T. M. Kranz, A. Berns, J. Shields, K. Rothman, J. Walsh-messinger, R. R. Goetz, M. V. Chao, and D. Malaspina, “EBioMedicine Phenotypically distinct subtypes of psychosis accompany novel or rare variants in four different signaling genes,” *EBIOM*, vol. 6, pp. 206–214, 2016.

[60] I. Kushima, B. Aleksic, M. Nakatochi, T. Shimamura, T. Okada, Y. Uno, M. Morikawa, K. Ishizuka, T. Shiino, H. Kimura, Y. Arioka, A. Yoshimi, Y. Takasaki, Y. Yu, Y. Nakamura, M. Yamamoto, T. Iidaka, S. Iritani, T. Inada, N. Ogawa, E. Shishido, Y. Torii, N. Kawano, Y. Omura, T. Yoshikawa, T. Uchiyama, T. Yamamoto, M. Ikeda, R. Hashimoto, H. Yamamori, Y. Yasuda, T. Someya, Y. Watanabe, J. Egawa, A. Nunokawa, M. Itokawa, M. Arai, M. Miyashita, A. Kobori, M. Suzuki, T. Takahashi, M. Usami, M. Kodaira, K. Watanabe, T. Sasaki, H. Kuwabara, M. Tochigi, F. Nishimura, H. Yamasue, Y. Eriguchi, S. Benner, M. Kojima, W. Yassin, T. Munesue, S. Yokoyama, R. Kimura, Y. Funabiki, H. Kosaka, M. Ishitobi, T. Ohmori, S. Numata, T. Yoshikawa, T. Toyota, K. Yamakawa, T. Suzuki, Y. Inoue, K. Nakaoka, Y.-i. Goto, M. Inagaki, N. Hashimoto, I. Kusumi, S. Son, T. Murai, T. Ikegame, N. Okada, K. Kasai, S. Kunimoto, D. Mori, N. Iwata, and N. Ozaki, "Comparative Analyses of Copy-Number Variation in Autism Spectrum Disorder and Schizophrenia Reveal Etiological Overlap and Biological Insights," *Cell Reports*, vol. 24, no. 11, pp. 2838–2856, 2018.

[61] J. P. Klooster and P. L. Hordijk, "Targeting and localized signalling by small GTPases," *Biology of the Cell*, vol. 99, no. 1, pp. 1–12, 2007.

[62] S. C. Borrie, H. Brems, E. Legius, and C. Bagni, "Cognitive Dysfunctions in Intellectual Disabilities: The Contributions of the Ras-MAPK and PI3K-AKT-mTOR Pathways," *Annual Review of Genomics and Human Genetics*, vol. 18, no. 1, pp. 115–142, 2017.

[63] D. J. Josifova, G. R. Monroe, F. Tessadori, E. de Graaff, B. van der Zwaag, S. G. Mehta, The DDD Study, M. Harakalova, K. J. Duran, S. M. C. Savelberg, I. J. Nijman, H. Jungbluth, C. C. Hoogenraad, J. Bakkers, N. V. Knoers, H. V. Firth, P. L. Beales, G. van Haaften, and M. M. van Haelst, "Heterozygous KIDINS220/ARMS nonsense variants cause spastic paraplegia, intellectual disability, nystagmus, and obesity," *Human Molecular Genetics*, vol. 25, no. 11, pp. 2158–2167, 2016.

[64] S. Ghosh and C. Bouchard, “Convergence between biological, behavioural and genetic determinants of obesity,” *Nature Reviews Genetics*, vol. 18, no. 12, pp. 731–748, 2017.

[65] I. L. Mero, H. H. Mørk, Y. Sheng, A. Blomhoff, G. L. Opheim, A. Erichsen, M. D. Vigeland, and K. K. Selmer, “Homozygous KIDINS220 loss-of-function variants in fetuses with cerebral ventriculomegaly and limb contractures,” *Human Molecular Genetics*, vol. 26, no. 19, pp. 3792–3796, 2017.

[66] F. Cesca, A. Yabe, B. Spencer-Dene, A. Arrigoni, M. Al-Qatari, D. Henderson, H. Phillips, M. Koltzenburg, F. Benfenati, and G. Schiavo, “Kidins220/ARMS is an essential modulator of cardiovascular and nervous system development,” *Cell Death and Disease*, vol. 2, no. 11, p. e226, 2011.

[67] Y. Lallemand, V. Luria, R. Haffner-Krausz, and P. Lonai, “Maternally expressed PGK-Cre transgene as a tool for early and uniform activation of the Cre site-specific recombinase.,” *Transgenic research*, vol. 7, no. 2, pp. 105–112, 1998.

[68] M. Lewandoski and G. R. Martin, “Cre-mediated chromosome loss in mice.,” *Nature genetics*, vol. 17, no. 2, pp. 223–225, 1997.

[69] A. M. Duffy, M. J. Schaner, S. H. Wu, A. Staniszewski, A. Kumar, J. C. Arévalo, O. Arancio, M. V. Chao, and H. E. Scharfman, “A selective role for ARMS/Kidins220 scaffold protein in spatial memory and trophic support of entorhinal and frontal cortical neurons,” *Experimental Neurology*, vol. 229, no. 2, pp. 409–420, 2011.

[70] G. Chen and H. K. Manji, “The extracellular signal-regulated kinase pathway: an emerging promising target for mood stabilizers,” *Current Opinion in Psychiatry*, vol. 19, no. 3, pp. 313–323, 2006.

[71] M. Masis-Calvo, A. Sequeira-Cordero, A. Mora-Gallegos, and J. Fornaguera-Trias, “Behavioral and neurochemical characterization of maternal care effects on juvenile Sprague-Dawley rats.,” *Physiology & behavior*, vol. 118, pp. 212–217, 2013.

[72] M. Ahn, D. Beacham, R. E. Westenbroek, T. Scheuer, and W. A. Catterall, “Regulation of NaV1.2 Channels by Brain-Derived Neurotrophic Factor, TrkB, and Associated Fyn Kinase,” *Journal of Neuroscience*, vol. 27, no. 43, pp. 11533–11542, 2007.

[73] P. Brennan and E. B. Keverne, “Biological complexity and adaptability of simple mammalian olfactory memory systems,” *Neuroscience and Biobehavioral Reviews*, vol. 50, pp. 29–40, 2015.

[74] H. Arakawa, D. C. Blanchard, K. Arakawa, C. Dunlap, and R. J. Blanchard, “Scent marking behavior as an odorant communication in mice.,” *Neuroscience and biobehavioral reviews*, vol. 32, no. 7, pp. 1236–1248, 2008.

[75] F. Bolz, S. Kasper, B. Bufe, F. Zufall, and M. Pyrski, “Organization and Plasticity of Sodium Channel Expression in the Mouse Olfactory and Vomeronasal Epithelia,” *Frontiers in Neuroanatomy*, vol. 11, pp. 1–15, 2017.

[76] K. G. Bath, N. Mandairon, D. Jing, R. Rajagopal, R. Kapoor, Z.-Y. Chen, T. Khan, C. C. Proenca, R. Kraemer, T. A. Cleland, B. L. Hempstead, M. V. Chao, and F. S. Lee, “Variant brain-derived neurotrophic factor (Val66Met) alters adult olfactory bulb neurogenesis and spontaneous olfactory discrimination.,” *The Journal of neuroscience : the official journal of the Society for Neuroscience*, vol. 28, no. 10, pp. 2383–2393, 2008.

[77] M. D. Kass, L. A. Czarnecki, A. H. Moberly, and J. P. McGann, “Differences in peripheral sensory input to the olfactory bulb between male and female mice,” *Scientific Reports*, vol. 7, pp. 1–15, 2017.

[78] K. R. Maynard, J. W. Hobbs, B. D. N. Phan, A. Gupta, S. Rajpurohit, C. Williams, A. Rajpurohit, J. H. Shin, A. E. Jaffe, and K. Martinowich, “BDNF-TrkB signaling in oxytocin neurons contributes to maternal behavior,” *eLife*, vol. 7, 2018.

[79] T. D. Purves-Tyson, K. Allen, S. Fung, D. Rothmond, P. L. Noble, D. J. Handelsman, and C. Shannon Weickert, “Adolescent testosterone influences BDNF and

TrkB mRNA and neurotrophin-interneuron marker relationships in mammalian frontal cortex," *Schizophrenia Research*, vol. 168, no. 3, pp. 661–670, 2015.

[80] J. N. Ferguson, L. J. Young, E. F. Hearn, M. M. Matzuk, T. R. Insel, and J. T. Winslow, "Social amnesia in mice lacking the oxytocin gene.," *Nature genetics*, vol. 25, no. 3, pp. 284–8, 2000.

[81] I. F. Bielsky, S. B. Hu, K. L. Szegda, H. Westphal, and L. J. Young, "Profound impairment in social recognition and reduction in anxiety-like behavior in vasopressin V1a receptor knockout mice," *Neuropsychopharmacology*, vol. 29, no. 3, pp. 483–493, 2004.

[82] T. Raam, K. M. McAvoy, A. Besnard, A. Veenema, and A. Sahay, "Hippocampal oxytocin receptors are necessary for discrimination of social stimuli," *Nature Communications*, vol. 8, no. 1, 2017.

[83] E. R. Bradley and J. D. Woolley, "Oxytocin effects in schizophrenia: Reconciling mixed findings and moving forward.," *Neuroscience and biobehavioral reviews*, vol. 80, pp. 36–56, 2017.

[84] K. M. Frick, J. Kim, J. J. Tuscher, and A. M. Fortress, "Sex steroid hormones matter for learning and memory: Estrogenic regulation of hippocampal function in male and female rodents," *Learning and Memory*, vol. 22, no. 9, pp. 472–493, 2015.

[85] L. M. Monteggia, M. Barrot, C. M. Powell, O. Berton, V. Galanis, T. Gemelli, S. Meuth, A. Nagy, R. W. Greene, and E. J. Nestler, "Essential role of brain-derived neurotrophic factor in adult hippocampal function," *Proceedings of the National Academy of Sciences, USA*, vol. 101, no. 29, pp. 10827–10832, 2004.

[86] F. W. Shum, S. W. Ko, Y. S. Lee, B. K. Kaang, and M. Zhuo, "Genetic alteration of anxiety and stress-like behavior in mice lacking CaMKIV," *Molecular Pain*, vol. 1, 2005.

[87] C. Montag, U. Basten, C. Stelzel, C. J. Fiebach, and M. Reuter, "The BDNF Val66Met polymorphism and anxiety: Support for animal knock-in studies from

a genetic association study in humans," *Psychiatry Research*, vol. 179, no. 1, pp. 86–90, 2010.

[88] B. J. Slater, K. A. Lenton, M. D. Kwan, D. M. Gupta, D. C. Wan, and M. T. Longaker, "Cranial sutures: a brief review.," *Plastic and reconstructive surgery*, vol. 121, no. 4, pp. 170e–8e, 2008.

[89] M. Tian, Y. Zeng, Y. Hu, X. Yuan, S. Liu, J. Li, P. Lu, Y. Sun, L. Gao, D. Fu, Y. Li, S. Wang, and S. M. McClintock, "7, 8-Dihydroxyflavone induces synapse expression of AMPA GluA1 and ameliorates cognitive and spine abnormalities in a mouse model of fragile X syndrome.," *Neuropharmacology*, vol. 89, pp. 43–53, 2015.

[90] U. Boltaev, Y. Meyer, F. Tolibzoda, T. Jacques, M. Gassaway, Q. Xu, F. Wagner, Y. L. Zhang, M. Palmer, E. Holson, and D. Sames, "Multiplex quantitative assays indicate a need for re-evaluating reported small-molecule TrkB agonists," *Science Signaling*, vol. 10, no. 493, 2017.

[91] M. Parrini, D. Ghezzi, G. Deidda, L. Medrihan, E. Castroflorio, M. Alberti, P. Baldelli, L. Cancedda, and A. Contestabile, "Aerobic exercise and a BDNF-mimetic therapy rescue learning and memory in a mouse model of Down syndrome.," *Scientific reports*, vol. 7, no. 1, p. 16825, 2017.

[92] F. L. Hitti and S. A. Siegelbaum, "The hippocampal CA2 region is essential for social memory," *Nature*, vol. 508, no. 7494, pp. 88–92, 2014.

[93] J. Bagley and L. Belluscio, "NIH Public Access," *Neuroscience*, vol. 169, no. 3, pp. 1449–1461, 2011.

[94] R. Li, X. Ma, G. Wang, J. Yang, and C. Wang, "Why sex differences in schizophrenia?," *Journal of translational neuroscience*, vol. 1, no. 1, pp. 37–42, 2016.

[95] H. Huang, C. Michetti, M. Busnelli, F. Manago, S. Sannino, D. Scheggia, L. Giancardo, D. Sona, V. Murino, B. Chini, M. L. Scattoni, and F. Papaleo, "Chronic

and acute intranasal oxytocin produce divergent social effects in mice.," *Neuropsychopharmacology : official publication of the American College of Neuropsychopharmacology*, vol. 39, no. 5, pp. 1102–1114, 2014.

[96] M. Yang and J. N. Crawley, "Simple Behavioral Assessment of Mouse Olfaction," no. July, pp. 1–12, 2009.

[97] F. Papaleo, L. Erickson, G. Liu, J. Chen, and D. R. Weinberger, "Effects of sex and COMT genotype on environmentally modulated cognitive control in mice.," *Proceedings of the National Academy of Sciences of the United States of America*, vol. 109, no. 49, pp. 20160–20165, 2012.